

Spring 2012

A submerged ocean wave energy converter

Xinwei Wang

University of New Hampshire, Durham

Follow this and additional works at: <https://scholars.unh.edu/thesis>

Recommended Citation

Wang, Xinwei, "A submerged ocean wave energy converter" (2012). *Master's Theses and Capstones*. 705.
<https://scholars.unh.edu/thesis/705>

This Thesis is brought to you for free and open access by the Student Scholarship at University of New Hampshire Scholars' Repository. It has been accepted for inclusion in Master's Theses and Capstones by an authorized administrator of University of New Hampshire Scholars' Repository. For more information, please contact nicole.hentz@unh.edu.

A SUBMERGED OCEAN WAVE ENERGY CONVERTER

BY

XINWEI WANG

BSCIE, Tianjin Institute of Urban Construction, 2005

THESIS

Submitted to the University of New Hampshire

In Partial Fulfillment of

The Requirements for the Degree of

Master of Science

In

Ocean Engineering

May, 2012

UMI Number: 1518010

All rights reserved

INFORMATION TO ALL USERS

The quality of this reproduction is dependent upon the quality of the copy submitted.

In the unlikely event that the author did not send a complete manuscript and there are missing pages, these will be noted. Also, if material had to be removed, a note will indicate the deletion.

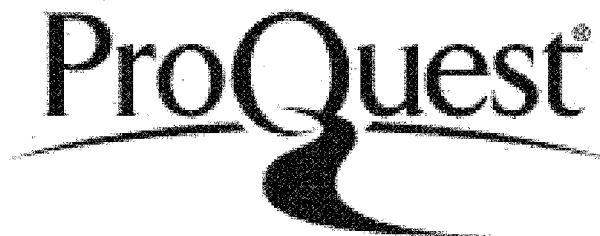


UMI 1518010

Published by ProQuest LLC 2012. Copyright in the Dissertation held by the Author.

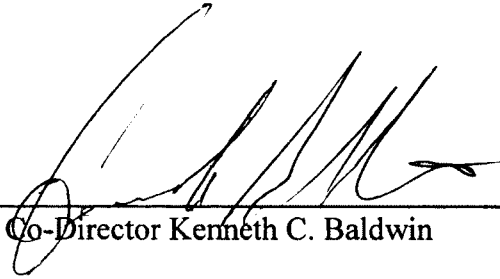
Microform Edition © ProQuest LLC.

All rights reserved. This work is protected against unauthorized copying under Title 17, United States Code.



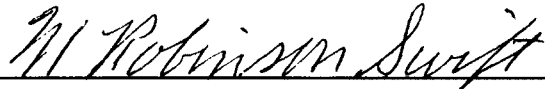
ProQuest LLC
789 East Eisenhower Parkway
P.O. Box 1346
Ann Arbor, MI 48106-1346

This thesis has been examined and approved.



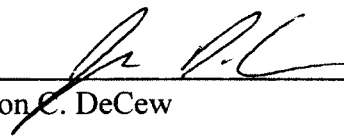
Thesis Co-Director Kenneth C. Baldwin

Professor of Mechanical and Ocean Engineering



Thesis Co-Director M. Robinson Swift

Professor of Mechanical and Ocean Engineering



Judson C. DeCew

Research Assistant Professor of Ocean Engineering

04/20/2012

Date

ACKNOWLEDGMENTS

I would like to thank Mr. John W. Rohrer, Principal of Rohrer Technologies Inc, as developer of the SOWEC G2 concept, he fabricated the physical scale model and all the enhancements.

Thanks to the funding source from: Maine Technology Institute, UNH CORE, Rohrer Technologies Inc.

Thanks to Professor Kenneth Baldwin for the opportunities he gave me to learn and study the renewable energy project. Also the scholarships for me evolved as a graduate student.

Thanks to Professor Robinson Swift, for his guidance and encouragement throughout this project. Judson DeCew, and all the members of the Chase Ocean Engineering Laboratory for their help and support.

TABLE OF CONTENTS

ACKNOWLEDGEMENTS.....	iii
TABLE OF CONTENTS.....	iv
LIST OF TABLES.....	vi
LIST OF FIGURES.....	vii
NOMENTCLATURE.....	viii
ABSTRACT.....	x
CHAPTER 1.....	1
Introduction	1
1.1 Background	1
1.2 Goals/Objectives	10
1.3 Approach	11
CHAPTER 2.....	12
Design	
2.1 Design concept	12
2.2 Major structure selected	14
2.2.1 Bellows.....	15
2.2.2 Piston water pump.....	16
2.2.3 Aluminum frame.....	17
2.2.4 Restoring force mechanism.....	18
2.3 Enhancements structure considered	19
2.3.1 Kinetic control surface.....	20
2.3.2 Extension plate.....	21
2.3.3 Shoal plane.....	22
2.4 Bellows expansion force-deflection measurement	23
2.5 SOWEC G-2 power estimation	25
2.5.1 Bellows full stroke compression power.....	27
2.5.2 Full ellipse stroke power.....	29
CHAPTER 3.....	32
Testing	
3.1 Testing objectives	32
3.2 Wave tank operation limitation	32
3.3 Equipment set up	33
3.4 OPIE & wave staff for measurement	34
3.4.1 OPIE.....	34
3.4.2 Wave staff.....	36
3.5 Preliminary Testing	37
3.6 Testing plan	39
CHAPTER 4.....	40
Experiment Data Processing and Results	
4.1 Efficiency calculation	40
4.1.1 Peak pressure method for determining output power	42
4.1.2 Average pressure times flow rate method for determining output Power.....	44
4.1.3 Comparison of the output power and estimated power.....	49

4.2	Experimental data analysis and evaluation	51
4.3	Experimental input power calculation	57
4.4	Full scale power prediction using Froude scaling	63
4.5	Performance improvement analysis	65
4.5.1	Stroke limitation.....	65
4.5.2	Piston water pump.....	65
4.5.3	PTO pressure.....	66
4.5.4	Restoring force.....	66
4.5.5	Enhancement structures.....	66
CHAPTER 5	67
	Conclusion	
5.1	Discussion of results	67
5.2	Future work	69
REFERENCES	70
APPENDIX A: REGULAR WAVE MODEL TEST RESULTS	71
APPENDIX B: SURFACE ELEVATION MEASURED BY WAVE STAFF	78

LIST OF TABLES

TABLE 2.1: Bellows Full Stroke Compression Power Estimation	28
TABLE 2.2: Full Ellipse Stroke Power Estimation	31
TABLE 3.1: Wave Tank Operation Limitation	32
TABLE 3.2: Testing Configuration Plan	39
TABLE 4.1: Peak Power Efficiency Results	43
TABLE 4.2: Average Power Efficiency Results	48
TABLE 4.3: Comparison of Estimated Power and Measured Output Power	50
TABLE 4.4: Open Ocean Wave Conditions Prediction	63

LIST OF FIGURES

Figure 1.1: U.S. Energy Consumption by Energy Source, 2008	2
Figure 1.2: U.S. Energy Consumption by Energy Source, 2009	2
Figure 1.3: U.S. Net Electricity Generation by Fuel, 2010	3
Figure 1.4: Oscillating Water Column (OWC)	4
Figure 1.5: Point Absorber	5
Figure 1.6: Overtopping Wave Energy Device	6
Figure 1.7: SOWEC G-1 Design	8
Figure 1.8: SOWEC G-2 Concept	9
Figure 2.1: SOWEC G-2 Design	12
Figure 2.2: Major Structure	14
Figure 2.3: Flexible Bellows	15
Figure 2.4: Piston Water Pump Work Flow	16
Figure 2.5: Aluminum Frame	17
Figure 2.6: Weight Restoring Force Mechanism	18
Figure 2.7: Enhancement Structures Evaluated in the Wave Experimental Program	19
Figure 2.8: Kinetic Control Surface	20
Figure 2.9: Extension Plate	21
Figure 2.10: Shoal Plane	22
Figure 2.11: Bellows Expansion Force-deflection Measurement	23
Figure 2.12: Bellows Expansion Force-deflection Measurement Result	24
Figure 2.13: Bellows Full Stroke Displacement with 9 inches	27
Figure 2.14: Elliptical Form of Water Particle Trajectory	29
Figure 3.1: Preliminary Testing	33
Figure 3.2: Overview of All Equipments Set Up	33
Figure 3.3: OPIE System	34
Figure 3.4: OPIE System Targets Dots on the Float and the Bellows Kinetic Control Surface	35
Figure 3.5: Wave Staff	36
Figure 3.6: Horizontal Orientation	37
Figure 3.7: Upward Orientation	38
Figure 3.8: Downward Orientation	38
Figure 4.1: Pressure fluctuation graphical definition	45
Figure 4.2: Flow Through the Orifice Inside the Pipe	45
Figure 4.3: Efficiency VS Depth	51
Figure 4.4: Efficiency VS Slope Angle	52
Figure 4.5: Efficiency VS Orientation	53
Figure 4.6: Efficiency VS Wave period	54
Figure 4.7: Efficiency VS Enhancement	55
Figure 4.8: OPIE Tracking System.	57
Figure 4.9: Bellows Pressure Plate Displacement VS. Surface Elevation(Aug.08#04)	58
Figure 4.10: Surface Elevation and Bellows Pressure Plate Horizontal Displacement Mathematical Model	59
Figure 4.11: Bellows Pressure Plate Displacement VS. Surface Elevation(Aug.08 #22)	61
Figure 4.12: Bellows Pressure Plate Displacement VS. Surface Elevation(Aug 16 #03)	62

NOMENCLATURE

Symbol	Description
m	Mass
ρ	Density
g	Gravitational constant
T	Period
η	Water surface elevation
k	Wave number
H	Wave height
L	Wave length
t	Time
F	Wave force
K_p	Pressure response factor
z	Vertical coordinate
σ	Relate radian frequency
δ_b	Bellows maximum compress displacement
ρ_{max}	Water maximum particle displacement in horizontal direction
ζ	Water particle displacement in horizontal direction
ξ	Water particle displacement in vertical direction
Z_c	Efficiency
W_e	Wave power
W_b	Bellows full stroke power
W_p	Ellipse full stroke power
W_{op}	Peak output power
W_{oa}	Average output power
W	Wave power applied to device
W_a	Average wave power applied to device
P	Instantaneous pressure
P_d	Dynamic pressure
P_l	Visual pressure gauge recorded pressure
P_{ave}	Average pressure
P_{max}	Maximum pressure from Visual pressure gauge
P_{min}	Minimum pressure from Visual pressure gauge
a	Pressure fluctuation amplitude
Q	Volumetric flow rate
Q_{ave}	Average volumetric flow rate
\mathcal{F}	Wave energy flux
b	Structure width
E	Total average energy per unit surface area
C_g	Group velocity
C	Wave celerity
C_o	Discharge coefficient
A	Orifice section area
A_p	Pressure plate area

A_i	Section area of output flow pipe
A_o	Section area of orifice
x	Distance bellows moves inward relative to its full expansion position
$(Fr)_p$	Prototype Froude number
$(Fr)_m$	Scale model Froude number
V	Velocity
$[W]_{dim}$	Device output power
$[W]_p$	Prototype output power
$[W]_m$	Model measured output power

ABSTRACT

A SUBMERGED OCEAN WAVE ENERGY CONVERTER

By

Xinwei Wang

University of New Hampshire, May 2012

The design of a Submerged Ocean Wave Energy Converter (SOWEC) was developed and evaluated using physical models in the University of New Hampshire (UNH) wave tank. The SOWEC is a unique “pumping” device and was designed to capture both potential (heave) energy and the kinetic (surge) energy from waves. The testing was done with a 1:8 scale model in the Chase Laboratory wave tank where it was subjected to regular (single frequency) waves having the maximum wave heights available for each period. The SOWEC was deployed at different depths and angles, with and without flow control attachments to enhance performance. A piston water pump was used as the power take-off system in this testing. Scale model peak pressure mechanical efficiencies up to 40 % were achieved in the model depending on operating configuration.

CHAPTER 1

INTRODUCTION

1.1 Background

The increase in worldwide consumption of fossil fuels continues to grow, amplifying pollution concerns. To protect limited resources and the environment, most of the world's countries have recently turned to renewable energy. Government agencies and private business have researched the potential of renewable sources of energy, increasing the investment thus accelerating the pace of innovation. A lot of manpower and resources have been invested to discover new renewable energy sources, develop resource planning, and organize practical projects to test technology.

Most renewable energy is eventually converted to electrical power for world energy consumption. In 2008 (Fig 1.1), renewable sources of energy were used to produce almost 7% (34% from hydropower and 66% from solar, geothermal, biomass and wind) of net electricity generated in the United States. In 2009 (Fig 1.2), renewable sources of energy increased to produce almost 8% (35% from hydropower and 65% from other renewable energy) of net electricity generated in the U.S. In 2010 (Fig 1.3), renewable sources of electricity production further were 10% (6% of total from hydropower and 4% from other renewable) of net electricity generated in the U.S. The

U.S. produces more electrical power from hydropower than the other renewable electricity resources.

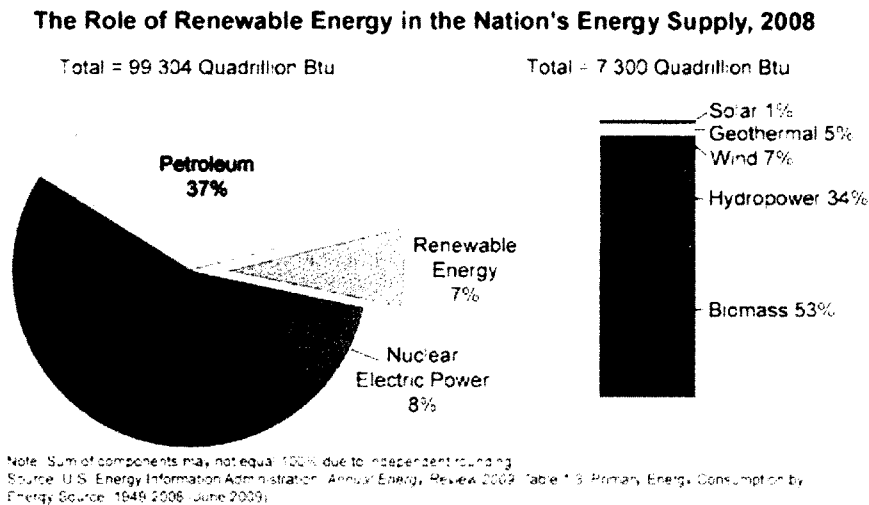


Figure 1.1 U.S. Energy Consumption by Energy Source, 2008. (U.S. Energy Information Administration, 2009)

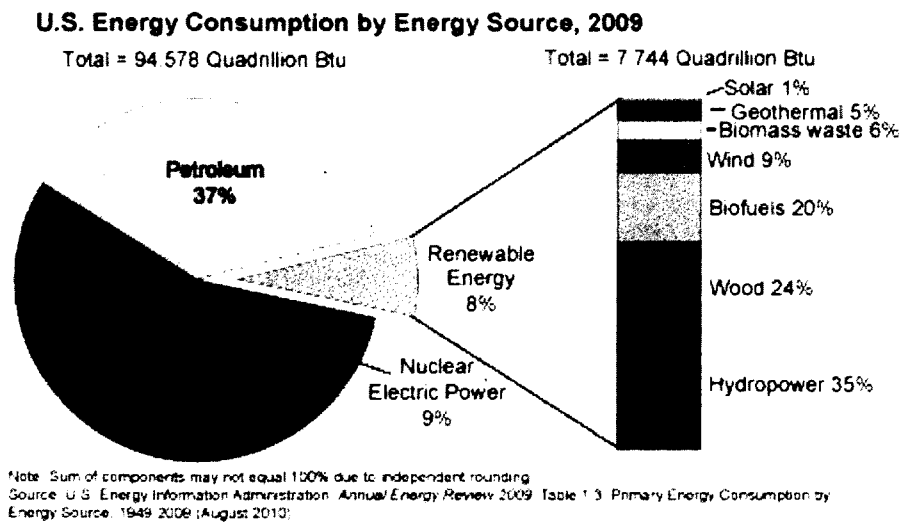
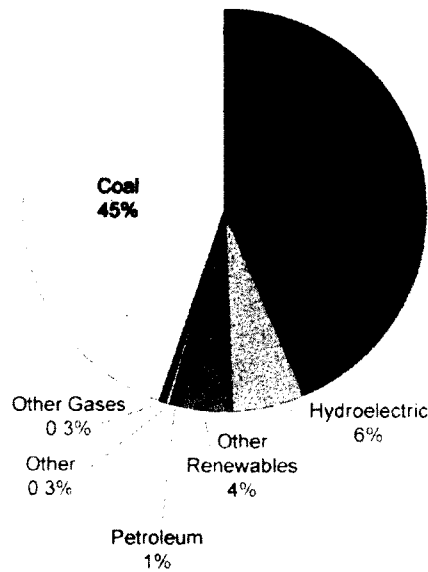


Figure 1.2 U.S. Energy Consumption by Energy Source, 2009. (U.S. Energy Information Administration, 2009)

U.S. Net Electricity Generation by Fuel, 2010



Source: U.S. Energy Information Administration, *Electric Power Monthly*, Table 1.1, preliminary data

Figure 1.3 U.S. Net Electricity Generation by Fuel, 2010. (U.S. Energy Information Administration, 2010)

Whereas the majority of alternative energy produced in the U.S. is by wind, solar and hydroelectric source, several designs have been proposed that harvests energy from ocean waves. With over 70% of the earth being covered by water, there is tremendous energy in the ocean waves. Wave energy could, therefore, play a very important role in future hydrokinetic energy development. The Electric Power Research Institute (EPRI) estimates that wave energy potential off the U.S. coast is roughly 252 million megawatt hours per year—equal to 6.5% of today’s entire generating portfolio and approximately the amount of baseload electricity presently produced by all traditional hydroelectric dams in the U.S. (The Ocean Renewable Energy Coalition, 2011).

With wave energy being an important source of renewable energy, the key challenge is how to extract the energy out from the wave efficiently. There are many wave energy conversion devices presently under development; most of them extract the potential energy of the waves.

The Oscillating Water Column device (Fig 1.4), for example, uses a large volume of moving water as a piston in a cylinder. Air is forced out of the column as a wave rises and fresh air is drawn in as the wave falls. This movement of air turns a turbine generator at the top of the column (John W. Twidell & Anthony D. Weir, 1986).

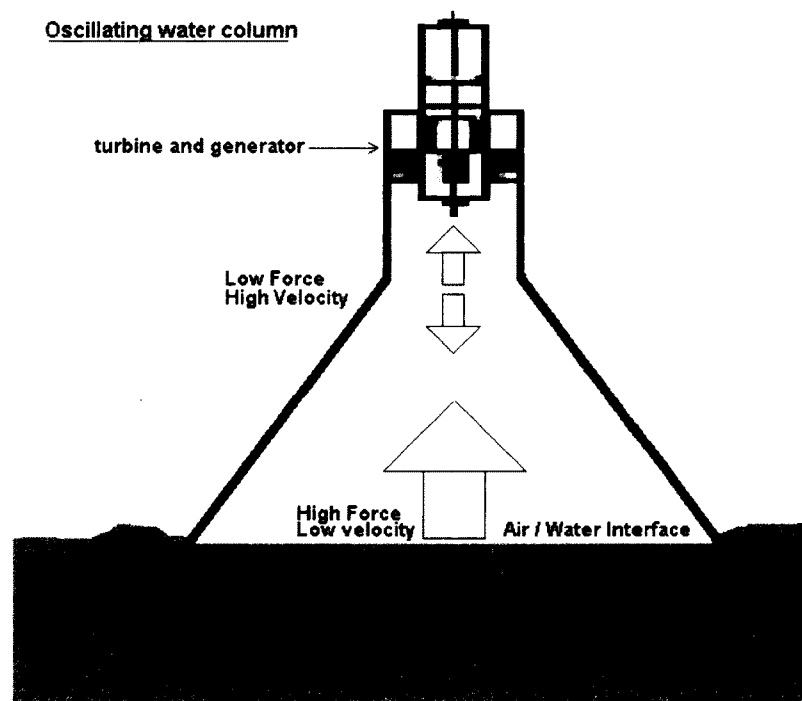


Figure 1.4 Oscillating Water Column (OWC). The cone-shaped structure is supported rigidly to the bottom.

The point absorber shown in Fig 1.5 consists of a buoy coupled directly to the rotor of a linear generator by a rope. The tension of the rope is maintained with a spring pulling the rotor downwards. The rotor moves up and down at approximately the same speed as the wave. The linear generator has a uniquely low pole height and generates electricity at low wave amplitudes and slow wave speeds (João Cruz, 2008).

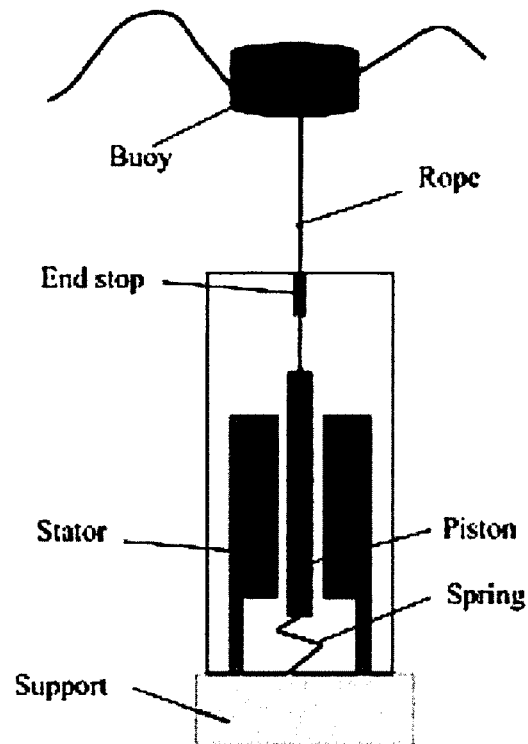


Figure1.5 Point Absorber

The overtopping wave energy device (Fig1.6) is a loosely anchored system that floats on the surface of the sea. It is usually anchored offshore to catch the highest waves. It has two wave reflectors which guide the waves toward a ramp which allows the waves to encroach and fill a reservoir with seawater. When the reservoir fills, the seawater drains through a large pipe housing a Kaplan turbine to generate power (João Cruz, 2008).

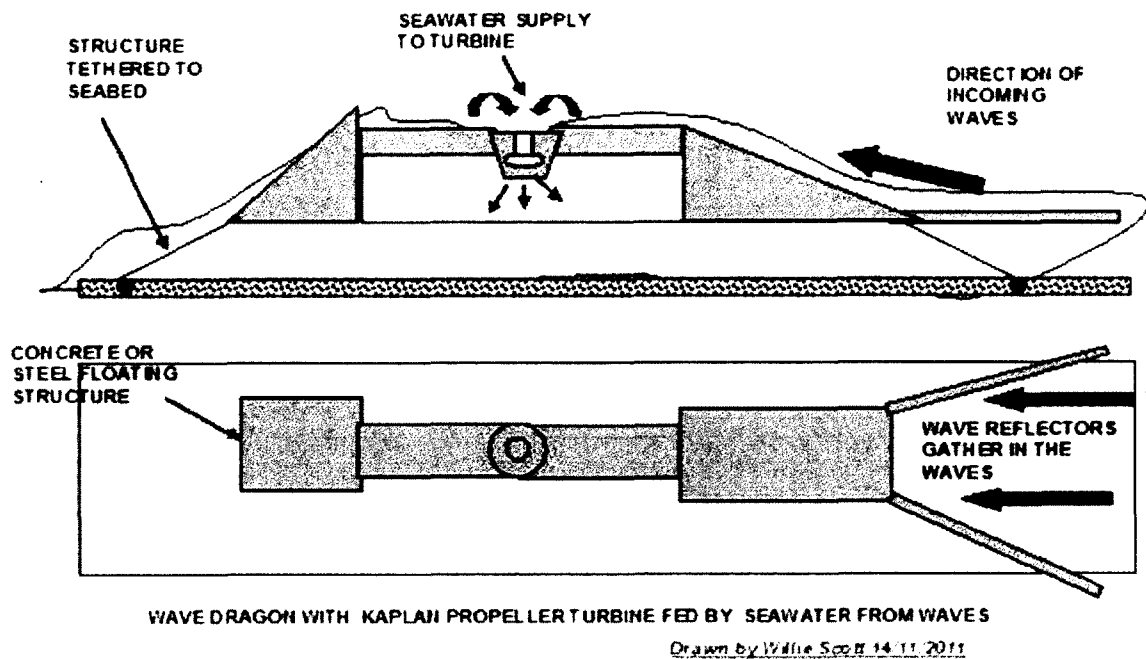


Figure1.6 Overtopping Wave Energy Device

These wave energy converter devices (oscillating water column, point absorber, overtopping device) are heave only structures which can only absorb the potential energy in the ocean wave energy. One limiting aspect of these systems are that they do not harvest the kinetic energy of the wave. Another disadvantage of the above device is that the upfront cost is significant. Most green energy harvesting devices have significant capital costs, whereas the maintenance or day to day operations are manageable. Because of this, many organizations are hesitant to invest in wave power plants.

To overcome these challenges, a Submerged Ocean Wave Energy Converter (SOWEC) was developed by Rohrer Technologies Inc. (RTI) to achieve multidirectional energy absorption at a reduced cost. To extract as much wave energy as possible, the concept is intended to capture both potential (heave) and kinetic (surge) wave energy. The device can be arranged as a line absorber or a point absorber, simplify the installation of maintenance requirements. In consideration of the real working condition in open random sea environments, this device also reduces moving mass and dependence on a resonance situation.

The first generation of SOWEC G-1(Fig 1.7) was tested in 2009 at the Center for Ocean Renewable Energy (CORE) at the University Of New Hampshire (UNH). The SOWEC G-1 prototype consisted of a rigid spring-cylinder fixed on a steel frame totally immersed in water. Both the wave's heave and surge motion could compress the spring-cylinder to create air pressure which was used to drive a piston water pump to generate power. This behavior makes the SOWEC G-1 able to extract both potential and kinetic

energy. The SOWEC G-1 was tested at different orientations and wave conditions. The output power SOWEC G-1 generated, however, was significantly lower by than the expectation.

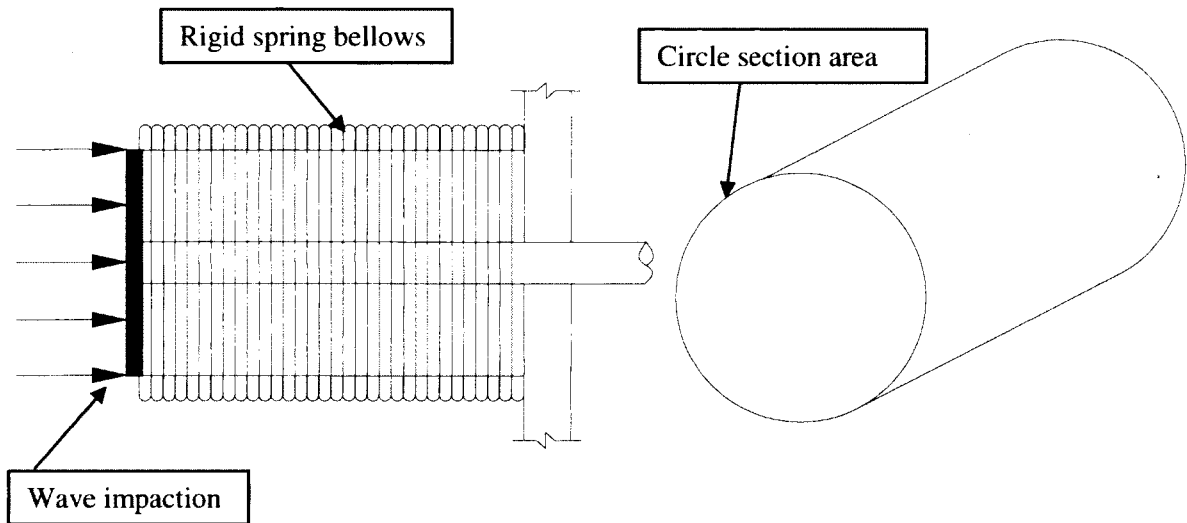


Figure 1.7 SOWEC G-1 Design

To increase the power output and efficiency of the system, a new design concept prototype SOWEC G-2 (Fig 1.8) was developed in summer 2011. A testing program was established to investigate its optimal operating characteristics. The SOWEC G-2 is a unique “pumping” device that was designed to capture both potential (heave) and kinetic (surge) wave energy, with low moving mass, over a wide band of wave periods. The SOWEC G-2 was not resonance dependent, ideal for random sea performance. New flexible material bellows replaced the rigid spring cylinder in SOWEC G-1. The flexible bellows pressure plate increased the absorbing area compared to the SOWEC G-1 cylinder section area. This device can also be connected to a variety power take-off systems (air turbine, hydraulic, rotary/linear generator) in future commercial designs.

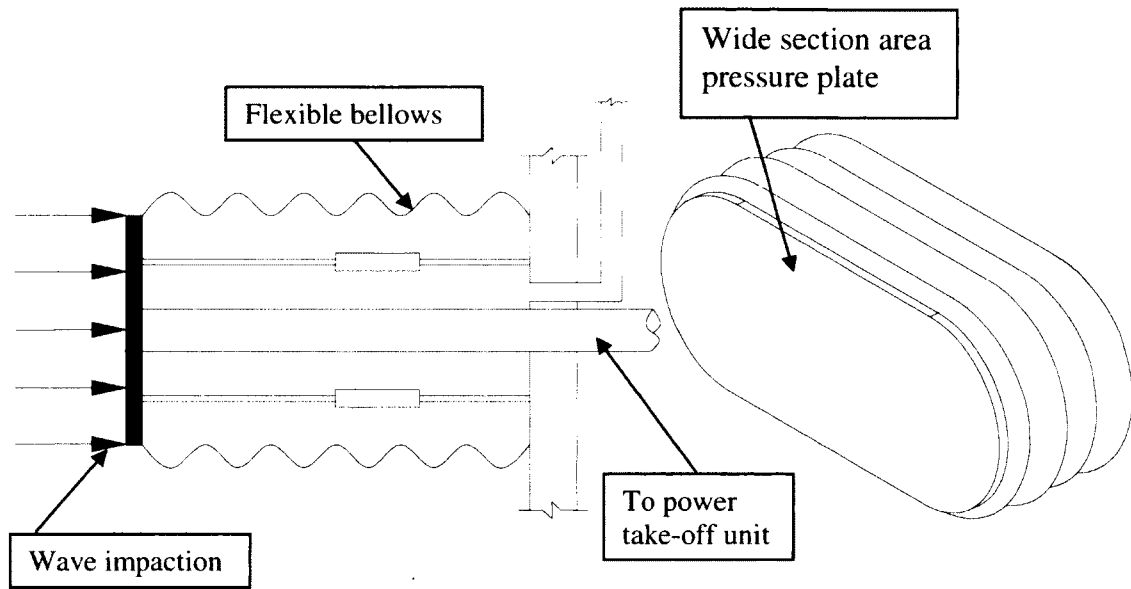


Figure 1.8 SOWEC G-2 Concept. This device consisted of flexible bellows and pressure plate. Power was generated through the power take-off unit when bellows pressure plate under the wave impaction.

1.2 Goals/Objectives

The goals of this research were:

1. Evaluate the design concept by experimental testing of an 1/8 commercial scale SOWEC G2 prototype.
2. Conduct parametric and performance testing at various submerged depths, slope angles, resistive force/loads, wave frequencies and amplitudes. Determine the SOWEC G-2 configuration with the highest energy output and the best wave conditions for optimal performance.
3. Measure effects of potential performance enhancements, including hydrodynamic wave impacting surfaces and wave shoaling and focusing means.
4. Develop effective testing protocols, data acquisition systems and data processing procedures for evaluating wave energy devices using physical models in the UNH wave tank.

1.3 Approach

A series of wave experiments were performed on the SOWEC G-2 to determine its performance for various wave environments and design configurations. Before in-water testing, however, bellows expansion force-deflection measurements were conducted to find out the bellows internal stiffness, which was important to optimize the required restoring force. In-water testing was done with a 1/8 scale model in the wave tank at UNH where it was subjected to regular (single frequency) waves having the maximum wave heights available for each period. The bellows motion response and output power were monitored. The SOWEC G-2 was deployed at different depths and angles, with and without flow control attachments to enhance performance. A piston water pump was used as the power take-off system. Flow from the pump was piped upward and released through an orifice. Pressure was recorded just upstream of the orifice, and the flow out was collected in a container. Pressure and volume flow rate were measured during the test to calculate the capture power of the device. Calculations of the available wave power were made so that the efficiency (capture power/ available power) of the SOWEC G-2 at this scale could be determined. The primary objective of this testing was to discover the SOWEC G-2 configuration with the highest energy output for the test wave condition. Analytical calculations of the device's capture power were made to estimate potential power output and for diagnostic purpose. In all cases analytical calculations were compared with direct measurements. Results were used to identify the best operating conditions and how the next generation SOWEC could be improved.

CHAPTER 2

Design

2.1 Design Concept

The SOWEC G-2 (Fig 2.1) was designed to capture wave energy by a flexible rubber bellows with a restoring force mechanism and a piston water pump as the power take-off system. When a wave crest propagates across the bellows, the increase in fluid pressure and surge impingement impacts on the pressure plate, compressing the bellows. The shaft inside the bellows transmits the force and motion to the power take-off system. After the wave crest passes the pressure plate, the restoring force mechanism inside the bellows drives the bellows expansion back to the initial position.

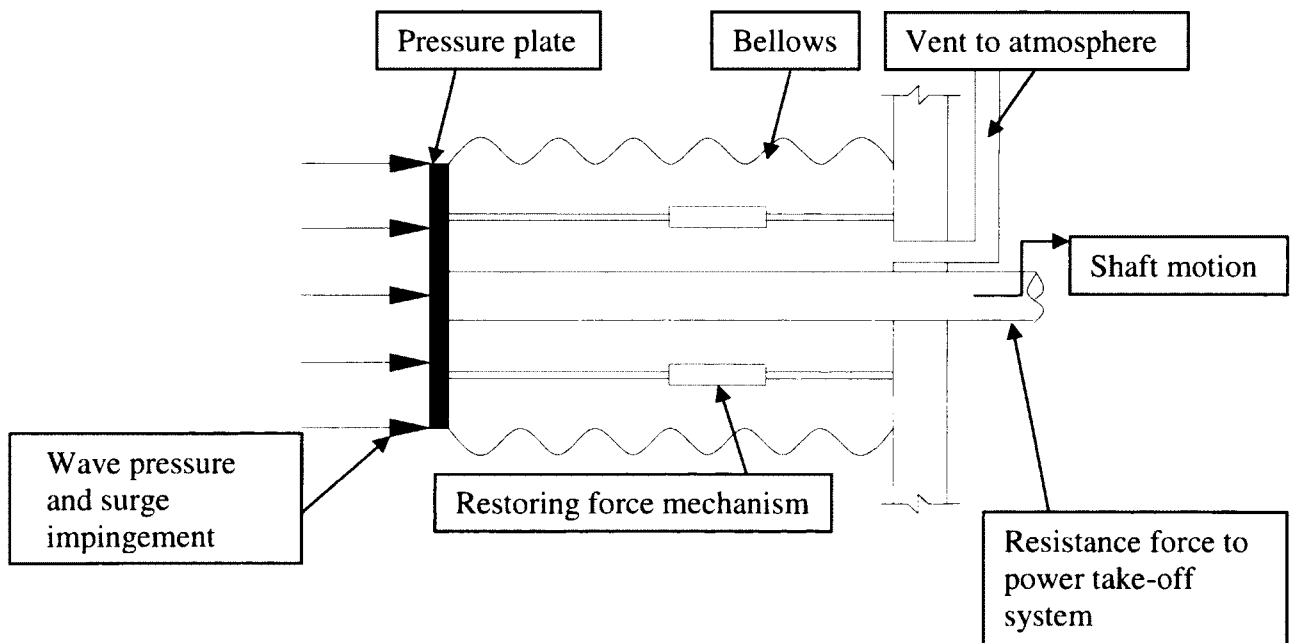


Figure 2.1 SOWEC G-2 Design

All high efficiency devices have the common characteristic that energy absorption is maximized and energy loss is minimized. To determine the optimal configuration for SOWEC G-2 performance, the bellows orientation and depth had to be adjustable to increase flow absorption. Note that, this conversion device should be suitable with any power take-off systems (air turbine, hydraulic, rotator /linear generator) in future development.

2.2 Major Structure Selected

A 1:8 scale model was made of a combination of components (Fig 2.2). These included a returnable rubber bellows, a restoring force mechanism, a piston water pump and an aluminum supporting frame. The bellows was made of flexible rubber material with inside guide rollers and supporting wires. The restoring force mechanism used in the testing consisted of a weight block connected via pulleys. However, the restoring force mechanism, in general, could consist of a spring, hydraulic, or constant weight mechanism. The entire basic structure (bellows, support frame and weights block) were assembled and mounted on the towing carriage in the UNH wave tank. The following sections describe each component in more detail.

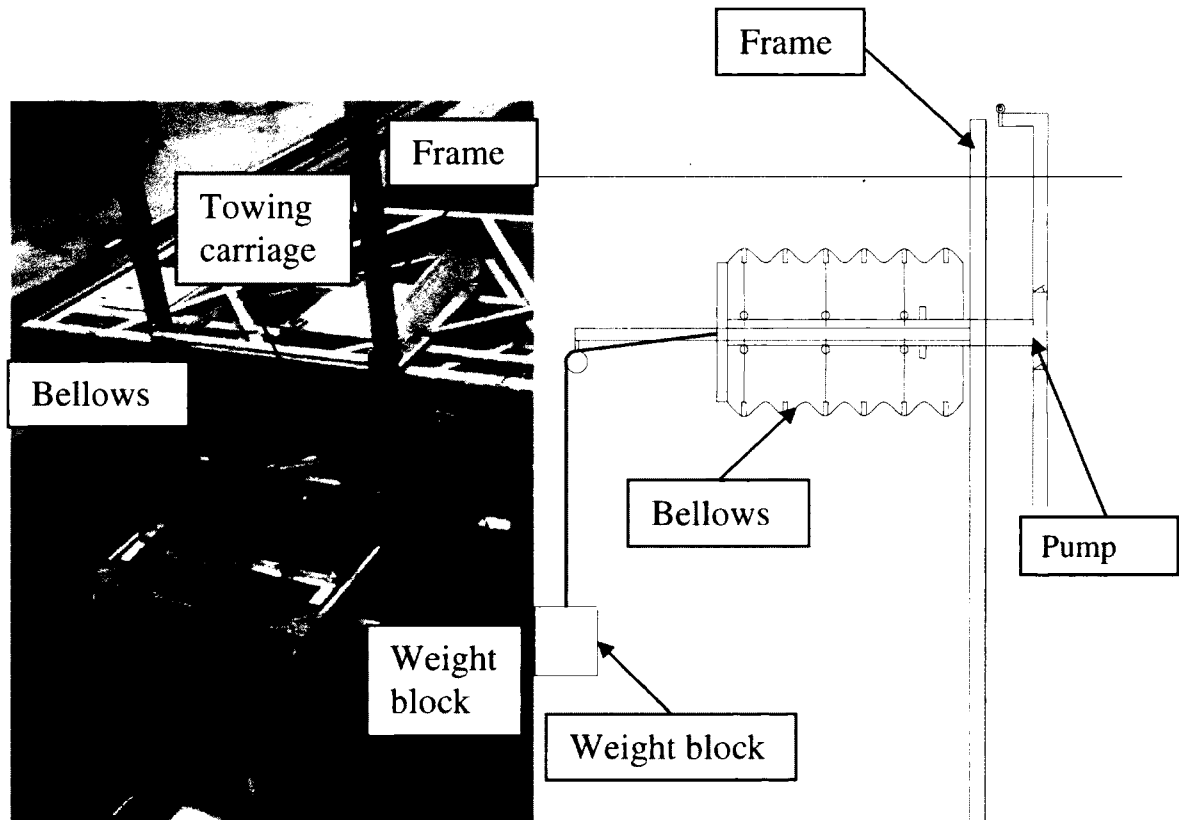


Figure 2.2 Major Structure

2.2.1 Bellows

The bellows (see Fig 2.3) was constructed out of flexible rubber material with wood ribs inside. Motion and deformation were controlled using guide rollers and supporting wires assembled inside the bellows. The bellows consisted of five composite materials layers. All inseams of the bellows were sealed by silicon. The geometric dimensions of the bellows are: 36 inches wide in the horizontal direction, 18 inches high in the vertical direction, length 15 inches (maximum) in the frontplate to backplate direction. Length can be fully extended (15 inches) or fully compressed (6 inches) with 9 inches stroke displacement. The rubber bellows was integrated with the front plate (pressure plate), backplate, and the aluminum support beam.

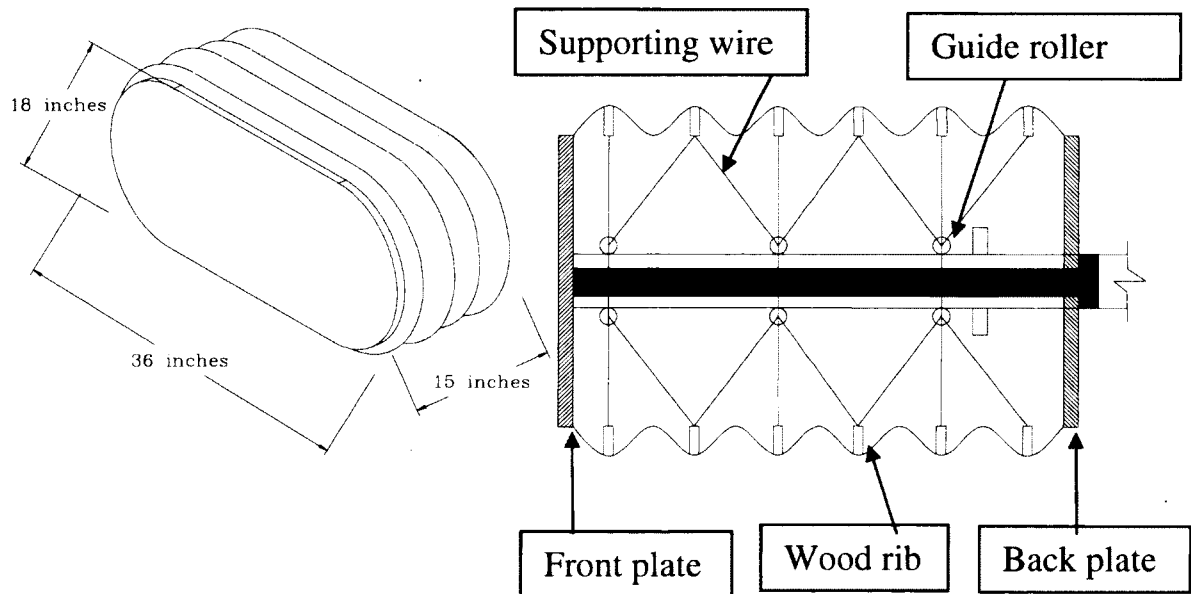


Figure 2.3 Flexible Bellows

2.2.2 Piston Water Pump

To evaluate mechanical power output, a monitored piston water pump (Fig 2.4) was used, which was located at the backside of the bellows. When the bellows was expanded by the restoring force system, the outside water pressure drove water into the piston water pump. When the bellows was compressed by wave impaction, the water in the pump was pushed by the piston up a vertical pipe through a one-way valve. The flow goes up to a measured height of 2.34 meters and out through an orifice plate directly. Water pressure was recorded by a visual pressure gauge before the water flows out through the orifice plate. The exit flow was collected in a container and the flow rate recorded. Note that, flow direction is controlled by the action of two one-way valves.

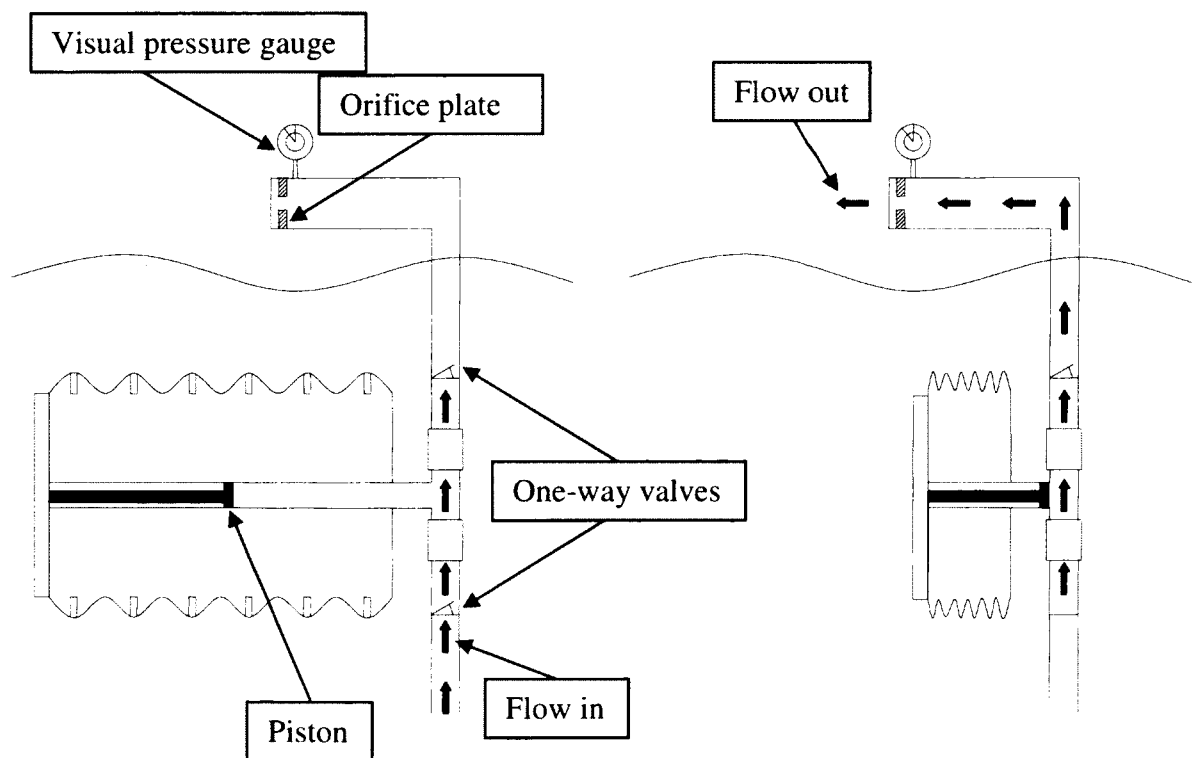


Figure 2.4 Piston Water Pump Work Flow

2.2.3 Aluminum Frame

The aluminum frame (Fig 2.5) consisted of two vertical rectangular hollow beams and three horizontal braces with the dimension of 10 feet height and 3.52 feet width. The bellows was fixed rigidly to the aluminum frame. The aluminum frame was attached to the towing carriage in the UNH wave tank. There were ten pairs of connection holes (2 inches interval spacing) in both sides of the aluminum frame to make both the depth and orientation of the bellows adjustable. This allowed the system to be submerged up to 1 meter.

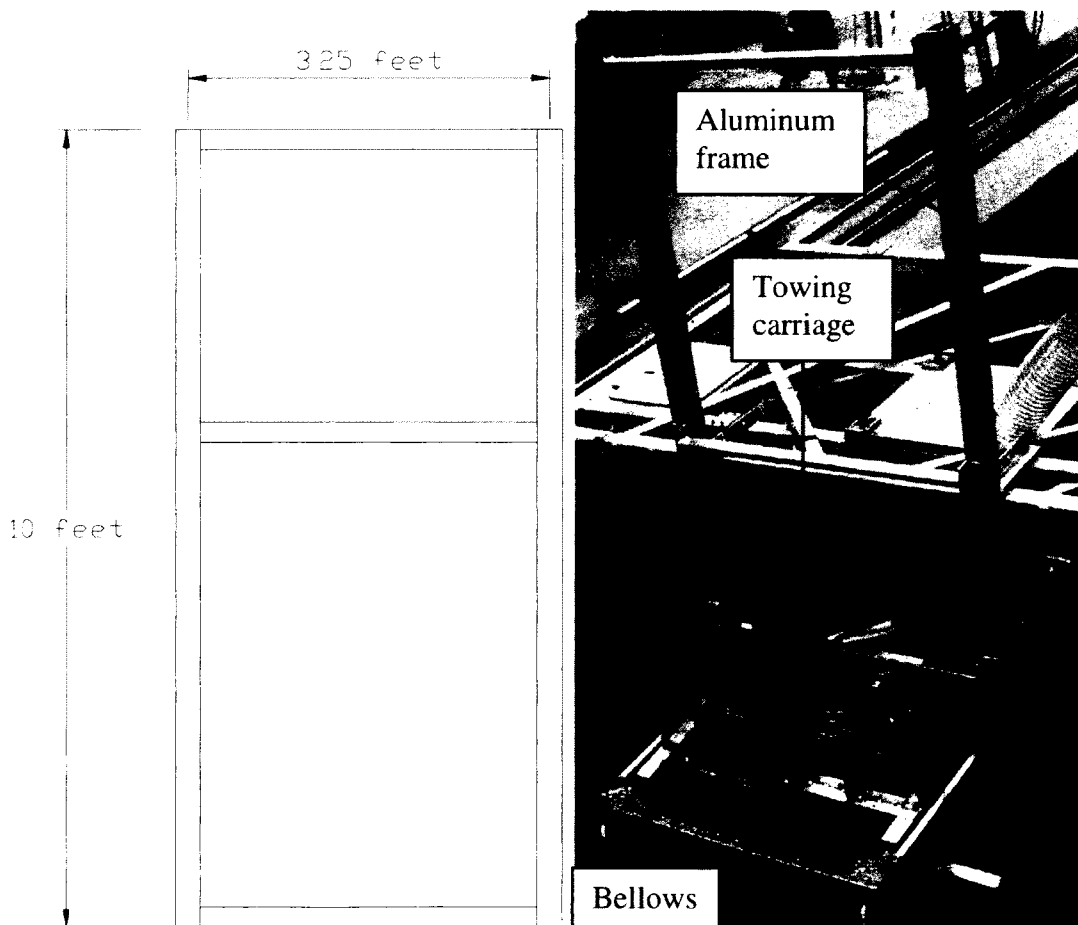


Figure 2.5 Aluminum Frame

2.2.4 Restoring Force Mechanism

Two pulley-weight arrangements (Fig 2.6) were used to supply constant-force restoring force mechanism. Weights consisted of five-pound blocks held in nylon nets.

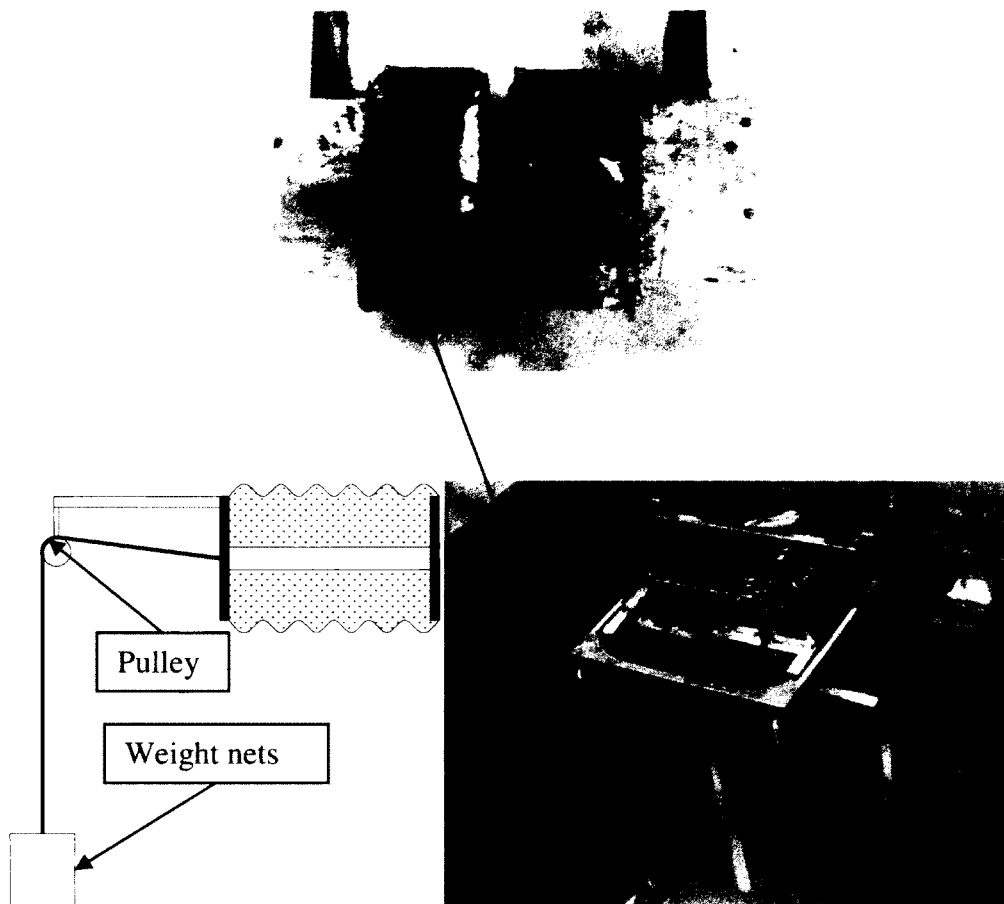


Figure 2.6 Weight Restoring Force Mechanism

2.3 Enhancement Structures Considered

To increase surge impact on the bellows front pressure plate, several enhancement structures (kinetic control surface, extension plate and shoal plane) were designed and fabricated. All structures used in the UNH wave tank experiments are shown in Fig 2.7. These devices were shaped to direct wave fluid motion towards the pressure plate. The enhancements are shown in more detail in the following sections.

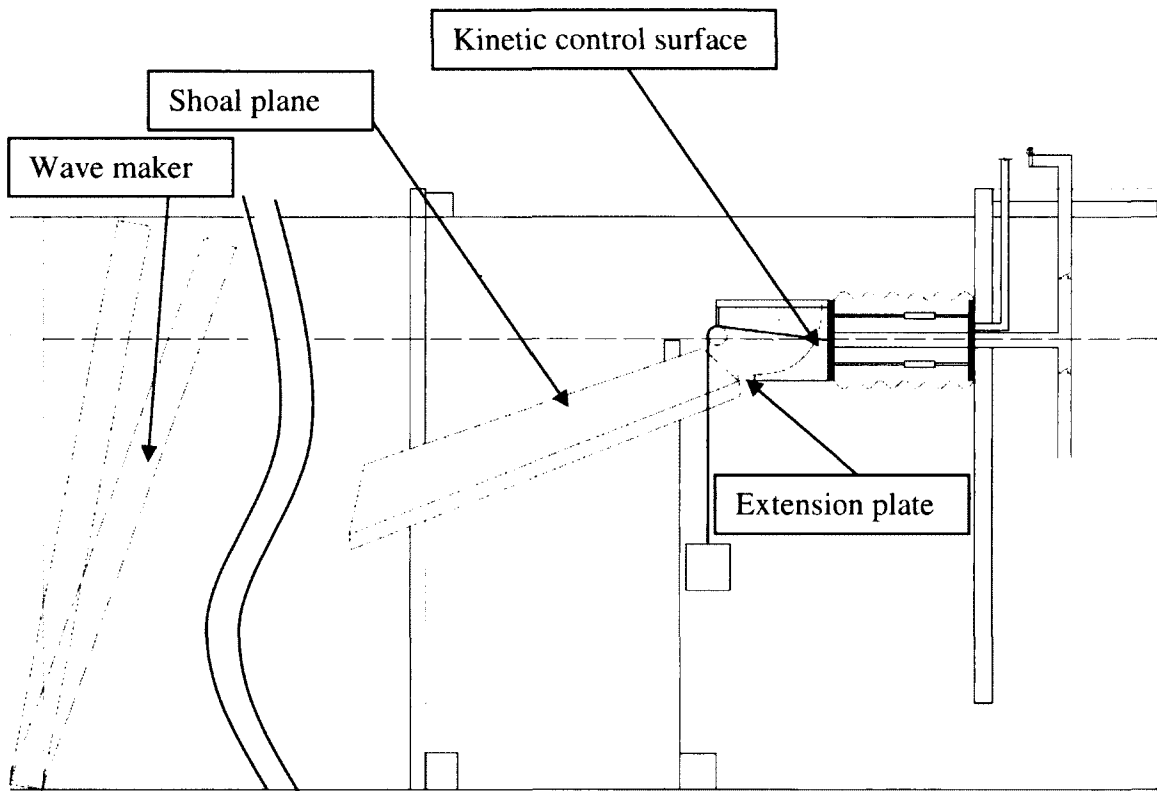


Figure 2.7 Enhancement Structures Evaluated in the Wave Experimental Program. Three enhancements are considered: kinetic control surface, extension plate and shoal plane.

2.3.1 Kinetic Control Surface

The kinetic control surface is the curved aluminum plate (36 inches wide and 20 inches along the curved length) which was bolted in front of the bellows pressure plate. The function of the kinetic control surface is to increase the wave pressure absorption area (about 20%) to gather more wave energy.

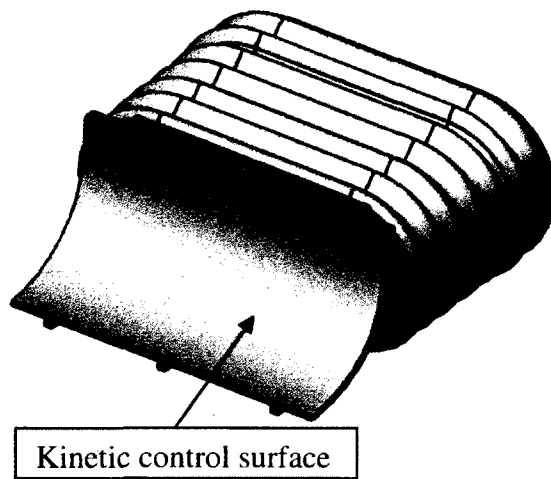


Figure 2.8 Kinetic Control Surface

2.3.2 Extension Plate

The extension plate (36 inches long and 18 inches wide) is the plate bolted to the base of the kinetic control surface to elongate its area(about 30%). The function of extension plate is to increase wave surge motion from below the device to impact the pressure plate.

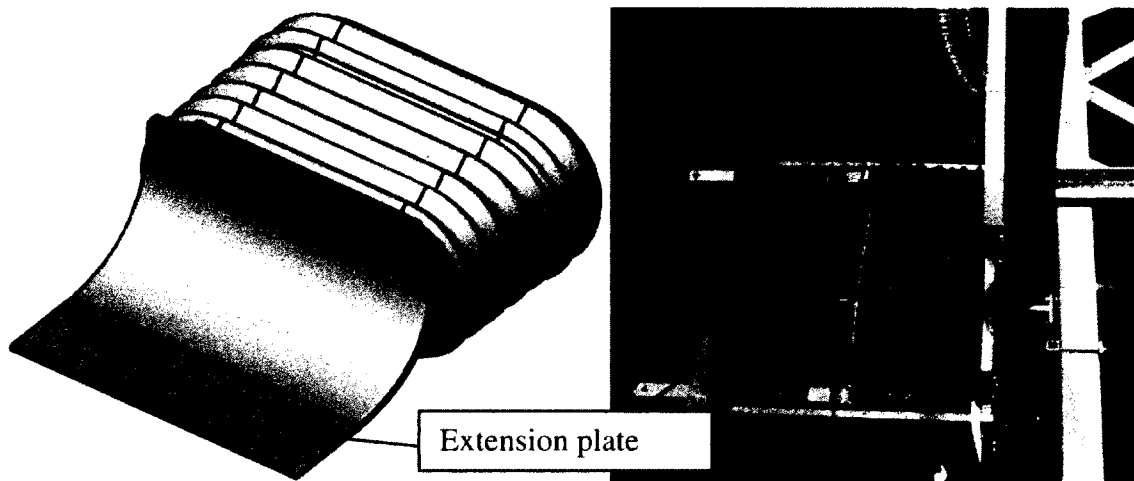


Figure 2.9 Extension Plate

2.3.3 Shoal Plane

The shoal plane (Fig 2.10) was designed to gather more dynamic pressure from lower wave layers and direct them to impact the bellows pressure plate. The shoal plane was made of plywood mounted on a vertical aluminum support foundation. Four aluminum vertical columns support the front and back end, and several crossing braces connect them to enhance structure strength. Four aluminum baskets were set up at the bottom ends of the vertical supports. Weight blocks were used to fill up the baskets to hold the frame fixed.

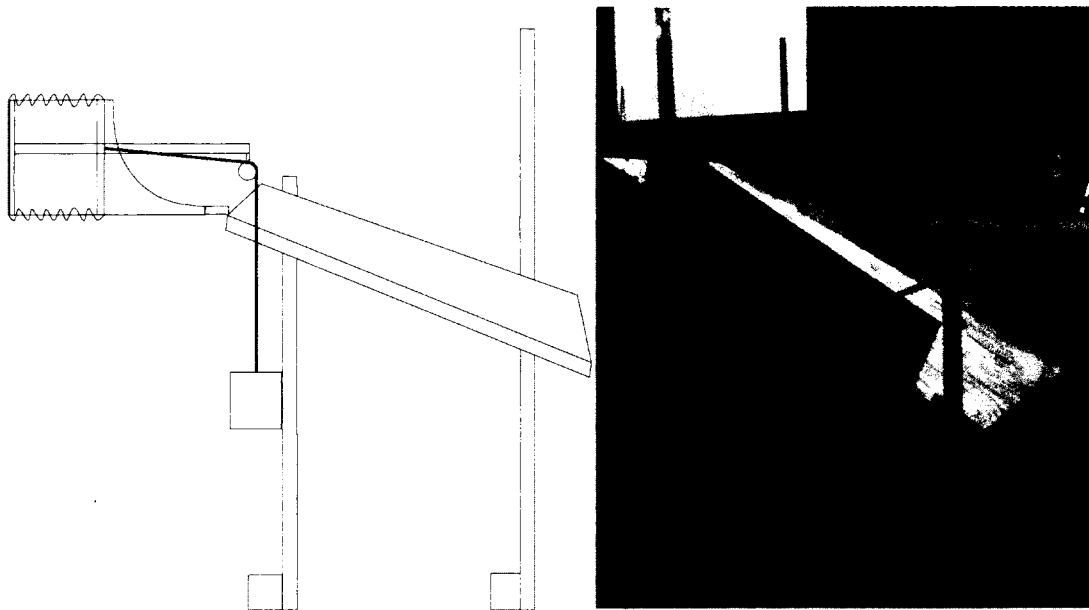


Figure 2.10 Shoal Plane. The shoal plane was at a slope of 30 degree, reached a depth of 6 feet, and was 4 feet wide.

2.4 Bellows Expansion Force-deflection Measurement

The first test conducted on the system examined the force required to expand the bellows. The bellows possessed internal stiffness that needed to be overcome by the pulley-weight system. To determine the size of the required weights, measurement of this force-deflection relationship was performed out-of-water, with no pump or pulley-weight attachment (Fig 2.11). The bellows was initially fully compressed, and then a tension force applied through a load cell to cause the bellows to expand. Measurement results are shown in Fig 2.12.

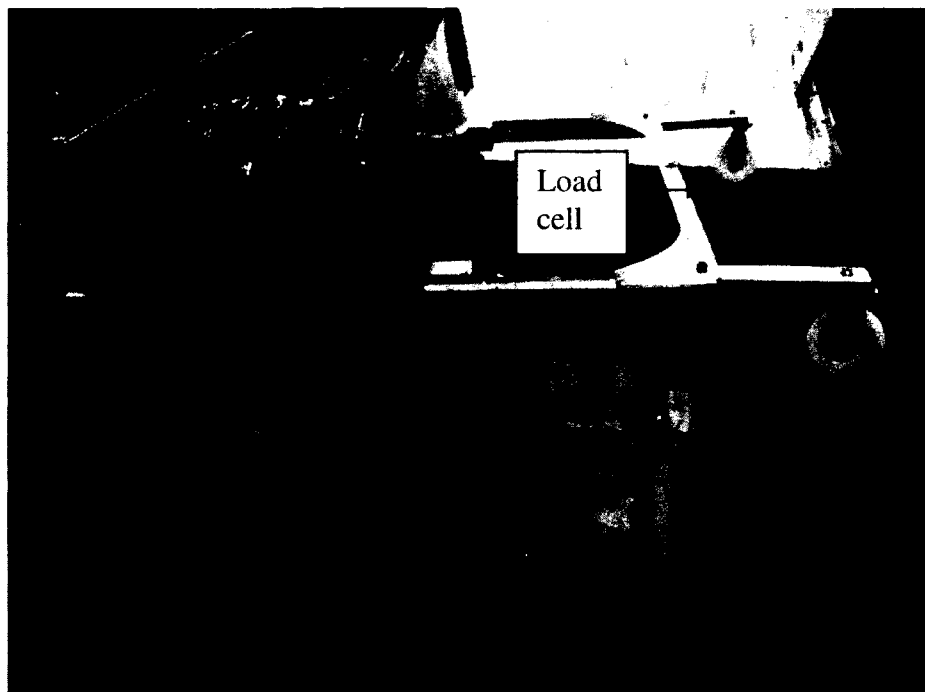


Fig 2.11 Bellows expansion force-deflection measurement

After the first experiments were done, the internal supports wires causing bellows stiffness were cut, and the bellows expanded freely. This test was used to select the ideal weights for each test to optimize the system response, and ranged for a fill at 60lbs to 140lbs.

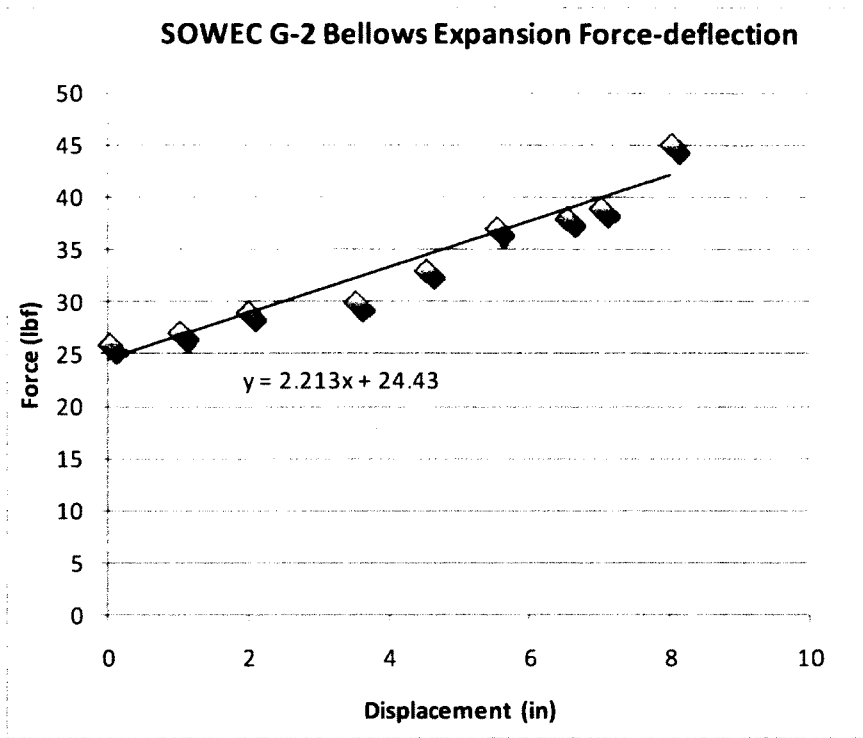


Figure 2.12 Bellows Expansion Force-deflection Measurement Result

2.5 SOWEC G-2 Power Estimation

Before the testing program was initiated, the device power was estimated for each planned experiment. To calculate the power of the SOWEC G-2, two crucial components were needed- the force working on the bellows pressure plate and a characteristic displacement. The pressure field within the waves was directly related to the force calculation. The power was calculated as the wave pressure amplitude force acting on the pressure plate times the characteristic displacement divided by half the wave period. In one method, the characteristic displacement was the bellows stroke length (see section 2.5.1) , and in the second approach, wave orbit dimensions were used (see section 2.5.2) .

Fluid pressure oscillation and fluid motion impingement cause the pressure plate movement to make the SOWEC G-2 generate the output power. The pressure can be separated in two parts: static pressure and dynamic pressure. Static pressure is constant and does no net work, while dynamic pressure (P_d) is caused by the wave motion. The force can be calculated by

$$F = P_d * A_p, \quad (2.5.1)$$

where P_d is the dynamic pressure, and A_p is the pressure plate area.

The dynamic pressure P_d can be calculated as

$$P_d = \rho * g * \eta * K_p, \quad (2.5.2)$$

where ρ is fluid density, η is the surface elevation, g is gravitational acceleration and K_p is the pressure response factor.

K_p is given by

$$K_p = \frac{\cosh [k(h + z)]}{\cosh [kh]}, \quad (2.5.3)$$

where z is the vertical coordinate, h is the depth, k is wave number. Note that the vertical coordinate, z , can equal zero at surface and $-h$ at bottom. Therefore, the pressure response factor has the maximum value 1 at surface and the minimum $1/\cosh(kh)$ at the bottom. The wave number is

$$k = 2\pi/L, \quad (2.5.4)$$

where L is the wave length. Wave number is determined from the dispersion relation,

$$\sigma^2 = gk \tanh(kh), \quad (2.5.5)$$

in which radian frequency σ , represented by

$$\sigma = \frac{2\pi}{T}, \quad (2.5.6)$$

where T is wave period (Dean and Dalrymple, 1991).

Using this theory, the power estimates of the system utilizing the bellows full stroke and water particle horizontal displacement as the characteristic displacement can be obtained.

2.5.1 Bellows Full Stroke Compression Power

In this approach, the characteristic displacement was assumed to be the full stroke compression displacement of 9 inches (see Fig 2.13).

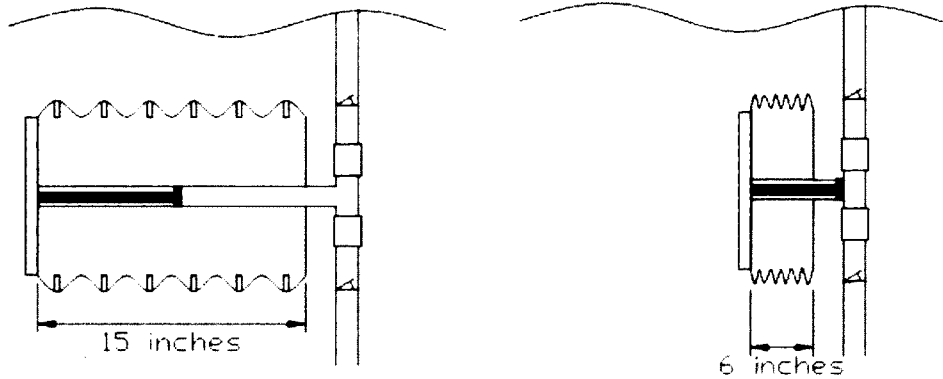


Figure 2.13 Bellows Full Stroke Displacement of 9 inches

The bellows full stroke power was estimated using the following relationship

$$W_b = \frac{F * \delta_b}{T/2} , \quad (2.5.7)$$

where F is the wave force (calculated from Equation 2.5.1), and δ_b is the bellows maximum compressive displacement of 9 inches. Results for wave environments and depths (-□, measured to the center of the pressure plate) planned for the test program are provided in Table 2.1.

Table 2.1 Bellows Full Stroke Compression Power Estimation

Bellows full stroke compression power estimation									
Below WL★	Period	Wave Length	Wave Height	Dynamic p	K _p	Pressure Area	Force	Distance	Estimate Power
Z _(m)	T _(s)	L _(m)	H _(m)	P _d (pascal)	factor	A _p (m ²)	F _(N)	δ _b (m)	W _b (watt)
-0.108	1.50	3.514	0.351	1419.555	0.825	0.288	408.832	0.229	124.830
-0.108	2.00	6.163	0.287	1263.166	0.897	0.288	363.792	0.229	83.308
-0.108	2.50	9.107	0.211	965.834	0.933	0.288	278.160	0.229	50.959
-0.133	1.50	3.514	0.351	1356.558	0.788	0.288	390.689	0.229	119.290
-0.133	2.00	6.163	0.287	1231.437	0.875	0.288	354.654	0.229	81.216
-0.133	2.50	9.107	0.211	950.362	0.918	0.288	273.704	0.229	50.143
-0.165	1.50	3.514	0.351	1281.731	0.744	0.288	369.139	0.229	112.710
-0.165	2.00	6.163	0.287	1192.933	0.847	0.288	343.565	0.229	78.676
-0.165	2.50	9.107	0.211	931.433	0.900	0.288	268.253	0.229	49.144
-0.191	1.50	3.514	0.351	1224.856	0.711	0.288	352.759	0.229	107.709
-0.191	2.00	6.163	0.287	1163.033	0.826	0.288	334.953	0.229	76.704
-0.191	2.50	9.107	0.211	916.612	0.886	0.288	263.984	0.229	48.362
-0.203	1.50	3.514	0.351	1197.373	0.695	0.288	344.844	0.229	105.292
-0.203	2.00	6.163	0.287	1148.376	0.816	0.288	330.732	0.229	75.738
-0.203	2.50	9.107	0.211	909.307	0.879	0.288	261.880	0.229	47.977
-0.229	1.50	3.514	0.351	1144.246	0.665	0.288	329.543	0.229	100.620
-0.229	2.00	6.163	0.287	1119.638	0.795	0.288	322.456	0.229	73.842
-0.229	2.50	9.107	0.211	894.907	0.865	0.288	257.733	0.229	47.217
-0.300	1.50	3.514	0.351	1007.213	0.585	0.288	290.077	0.229	88.570
-0.300	2.00	6.163	0.287	1042.816	0.741	0.288	300.331	0.229	68.776
-0.300	2.50	9.107	0.211	855.884	0.827	0.288	246.495	0.229	45.158
-0.500	1.50	3.514	0.351	704.743	0.409	0.288	202.966	0.229	61.972
-0.500	2.00	6.163	0.287	855.869	0.608	0.288	246.490	0.229	56.446
-0.500	2.50	9.107	0.211	757.354	0.732	0.288	218.118	0.229	39.959
-1.000	1.50	3.514	0.351	289.646	0.168	0.288	83.418	0.229	25.470
-1.000	2.00	6.163	0.287	531.253	0.377	0.288	153.001	0.229	35.037
-1.000	2.50	9.107	0.211	570.775	0.551	0.288	164.383	0.229	30.115

★ The depth of pressure plate center below the water level.

As seen in Table 2.1, the power estimates decreased with the depth of pressure plate for the same wave period. In general, the power ranged from 25 W to 125 W, with a mean power of 70 W for the selected load cases. The maximum estimated power generated was 125 W for a 1.5 second wave period, 0.351 meter wave height at a depth of 0.108 meter. These power estimates were used to compared with the measured capture power values, described in more detail in section 4.1.3, Table 4.3.

2.5.2 Full Ellipse Stroke Power

The elliptical form of water particle trajectory is shown in Fig 2.14 (Dean and Dalrymple, 1991) .

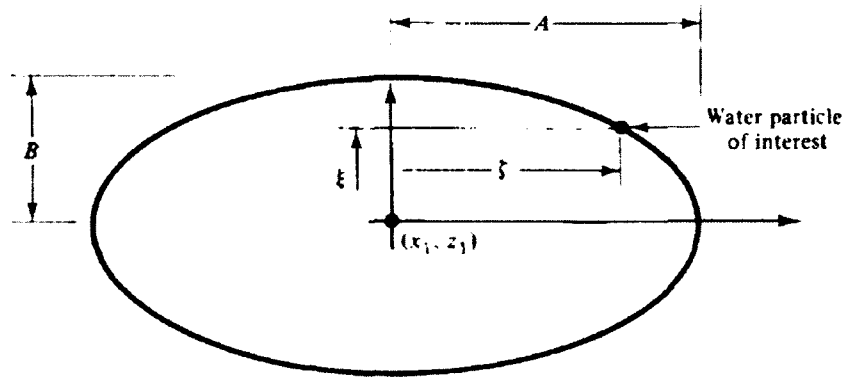


Figure 2.14 Elliptical Form of Water Particle Trajectory.

(A is the water particle maximum displacement in horizontal direction, B is the water particle maximum displacement in vertical direction.)

The second approach taken to estimate the power generation of the device utilized the wave water particle trajectory for the characteristic displacement. From linear wave theory, the horizontal and vertical displacement components of a water particle in waves are given by

$$\zeta = -\frac{H \cosh k(h+z) \sin(kx - \sigma t)}{2 \sinh(kh)}, \quad (2.5.8)$$

and

$$\xi = \frac{H \sinh k(h+z) \cos(kx - \sigma t)}{2 \sinh(kh)}, \quad (2.5.9)$$

where ζ is water particle horizontal displacement, ξ is water particle vertical displacement, t is time, x is horizontal coordinate.

In this second approach, the characteristic displacement is assumed to be $\zeta_{max} = A$, so that the ellipse full stroke power W_p can be calculated from

$$W_p = \frac{F * \zeta_{max}}{T/2}, \quad (2.5.10)$$

where F is the pressure force (calculated from Equation 2.5.1), ζ_{max} is the water particle displacement in horizontal direction (calculated from Equation 2.5.8). Estimates for test condition planned for the experimental program are provided in Table 2.2.

Table 2.2 Full Ellipse Stroke Power Estimation

Full ellipse stroke power estimation										
Below WL★	Period	Wave Length	Wave Height	Dynamic p	Ellip length	K _p	ΔPressure	Pressure Area	Force	Estimate Power
z _m (m)	T _(s)	L _(m)	H _(m)	P _d (pascal)	P _{max} (m)	factor	P _(pascal)	S _(m²)	F _(N)	W _p (watt)
-0.108	1.50	3.514	0.351	1419.555	0.145	0.825	2478.545	0.288	408.832	78.906
-0.108	2.00	6.163	0.287	1263.166	0.131	0.897	2322.156	0.288	363.792	47.497
-0.108	2.50	9.107	0.211	965.834	0.106	0.933	2024.823	0.288	278.160	23.479
-0.133	1.50	3.514	0.351	1356.558	0.138	0.788	2664.721	0.288	390.689	72.058
-0.133	2.00	6.163	0.287	1231.437	0.127	0.875	2539.600	0.288	354.654	45.141
-0.133	2.50	9.107	0.211	950.362	0.104	0.918	2258.526	0.288	273.704	22.733
-0.165	1.50	3.514	0.351	1281.731	0.131	0.744	2901.362	0.288	369.139	64.328
-0.165	2.00	6.163	0.287	1192.933	0.123	0.847	2812.564	0.288	343.565	42.362
-0.165	2.50	9.107	0.211	931.433	0.102	0.900	2551.064	0.288	268.253	21.836
-0.191	1.50	3.514	0.351	1224.856	0.125	0.711	3093.661	0.288	352.759	58.745
-0.191	2.00	6.163	0.287	1163.033	0.120	0.826	3031.838	0.288	334.953	40.265
-0.191	2.50	9.107	0.211	916.612	0.100	0.886	2785.417	0.288	263.984	21.147
-0.203	1.50	3.514	0.351	1197.373	0.122	0.695	3190.765	0.288	344.844	56.139
-0.203	2.00	6.163	0.287	1148.376	0.119	0.816	3141.768	0.288	330.732	39.257
-0.203	2.50	9.107	0.211	909.307	0.099	0.879	2902.699	0.288	261.880	20.811
-0.229	1.50	3.514	0.351	1144.246	0.117	0.665	3386.812	0.288	329.543	51.268
-0.229	2.00	6.163	0.287	1119.638	0.116	0.795	3362.204	0.288	322.456	37.317
-0.229	2.50	9.107	0.211	894.907	0.098	0.865	3137.473	0.288	257.733	20.157
-0.300	1.50	3.514	0.351	1007.213	0.103	0.585	3950.213	0.288	290.077	39.723
-0.300	2.00	6.163	0.287	1042.816	0.108	0.741	3985.816	0.288	300.331	32.372
-0.300	2.50	9.107	0.211	855.884	0.093	0.827	3798.884	0.288	246.495	18.438
-0.500	1.50	3.514	0.351	704.743	0.072	0.409	5609.743	0.288	202.966	19.448
-0.500	2.00	6.163	0.287	855.869	0.088	0.608	5760.869	0.288	246.490	21.805
-0.500	2.50	9.107	0.211	757.354	0.083	0.732	5662.354	0.288	218.118	14.437
-1.000	1.50	3.514	0.351	289.646	0.030	0.168	10099.646	0.288	83.418	3.285
-1.000	2.00	6.163	0.287	531.253	0.055	0.377	10341.253	0.288	153.001	8.401
-1.000	2.50	9.107	0.211	570.775	0.062	0.551	10380.775	0.288	164.383	8.200

★ The depth of pressure plate center below the water level.

Similar to the bellows stroke power estimate results, the power values decreased with depth of pressure plate for the same wave period. The maximum estimated power generated was 79 W for a 1.5 second wave with 0.351 meter wave height at a depth of 0.108 meter. These power estimates are compared with measured capture power in section 4.1.3, Table 4.3. The mean power for these experiments was found to be 34 W. It is important to note that these power estimates were lower than the bellows stroke displacement estimates due to the decrease characteristic displacement used in the calculations.

Chapter 3

Testing

3.1 Testing Objectives

A test program was carried out in the UNH wave tank to:

- Evaluate the device's power generation ability.
- Determine optimal operation configuration for the SOWEC G-2.
- Develop procedures and data acquisition hardware for evaluating wave energy collection devices using physical models in the UNH wave tank.

3.2 Wave Tank Operation Limitation

The wave tank is located in the Jere A. Chase Ocean Engineering Laboratory. Measuring 12' x 100' x 8' deep, wave creation is accomplished by using a hydraulic wave generator that can produce 0.5 to 3 second regular and irregular waves. The maximum wave height that can be generated is given for various wave periods in Table 3.1.

Table 3.1 Wave Tank Operation Limitation

Wave Periods (s)	Maximum Wave Height (m)
0.5	0.039
0.75	0.088
1.0	0.156
1.5	0.351
2	0.287
2.5	0.211
3	0.13

3.3

Equipment Set Up

All parts of the structure were assembled in the Chase Laboratory and mounted on the carriage which was fixed so that the device was opposite the observation window. During preliminary testing, only the bellows was mounted on the supporting aluminum frame (Fig 3.1). Preliminary testing consisted of running the device in waves and checking for leakage, jamming and preventable sources of friction. All other components and enhancements were added after preliminary testing (Fig 3.2).



Fig 3.1 Preliminary Testing



Figure 3.2 Overview of Complete Equipment Set Up

3.4 OPIE & Wave Staff for Measurement

3.4.1 OPIE

Accurately measuring surface elevation and bellows pressure plate movement was important for evaluating system performance. The Optical Positioning and Instrumentation Evaluation (OPIE) system was employed for this experiment. OPIE was originally developed to record an object's horizontal and vertical movement by using a digital camera to track the trajectory of a target dot fixed to the object (Fig 3.3). Movement of the target dot on a succession of image frames was used to compute displacement time series by Matlab software.

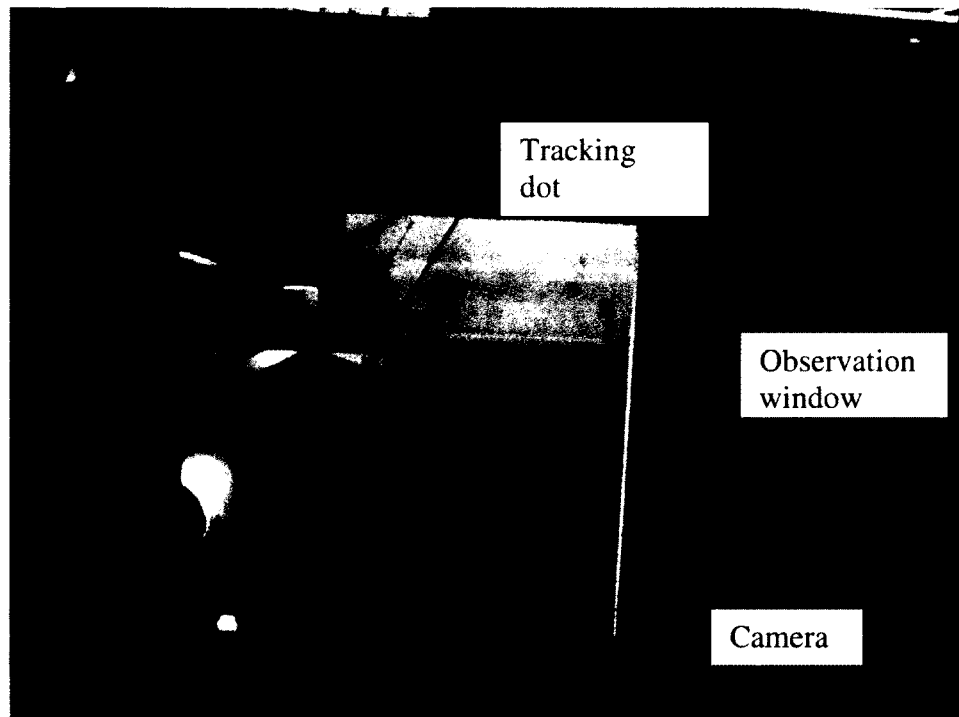


Figure 3.3 OPIE System. The digital camera views the system with target dots through the tank observation window.

The black dot on the white circle plate located on the bellows kinetic control surface (see Fig 3.4) was used to measure bellows displacement, and the black dot on the float was used to measure wave surface elevation. The buoyant float was constrained to move vertically along a taut, vertical wire. The black dots on the kinetic control surface and float were tracked at 30 Hertz for a duration of approximate 10 seconds in different wave conditions. The software then processed the images and provided the motion results of the tracked dots.

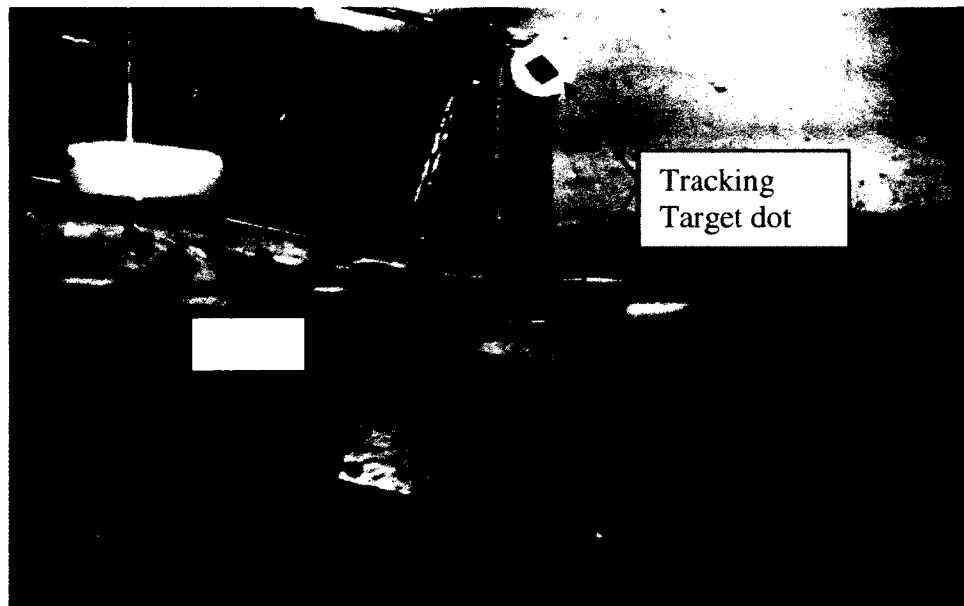


Figure 3.4 Target dots on the float (sliding on the vertical wire) and the bellows kinetic control surface.

3.4.2 Wave Staff

Since wave surface elevation measurement was crucial, a second method was used for redundancy and a check. A wave staff (Fig 3.5) is a reliable and accurate instrument for the measurement of surface elevation in the UNH wave tank. This twin-wire resistance probe was applied because of its ease of use and good dynamic performance. In operation, two parallel vertical wires are partly immersed in water and supplied with a constant voltage. If the depth of immersion is sufficiently large, the end effect is negligible, and the electrical conductance between the wires will be proportional to the depth of immersion and the water conductivity. Provided that the conductivity does not change, the electrical current flowing between the wires is a measure of the water surface elevation. A voltage time series was recorded during the wave testing. Voltage was converted to surface elevation using constants established through a calibration process. (Results are provided in Appendix B.)

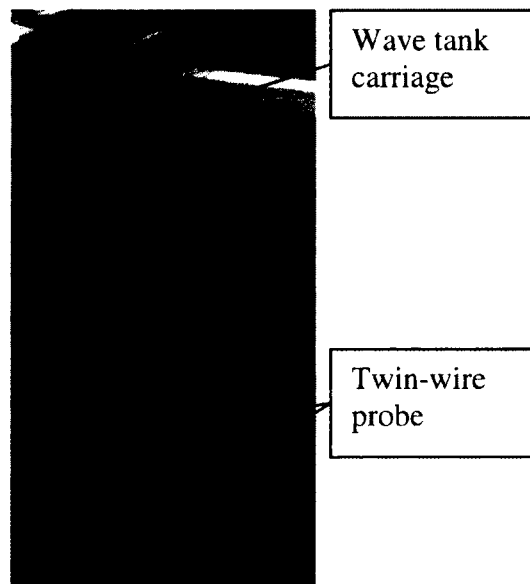


Figure 3.5 Wave Staff

3.5 Preliminary Testing

Before power output performance measurements were made, preliminary testing was conducted to check the operability of the basic physical scale model. Three different configurations (horizontal-Fig3.6, forward-Fig3.7 and downward-Fig3.8) were tested for bellows leakage and re-expansion ability under various wave conditions. The device was also submerged up to 1 meter and no leakage was observed.

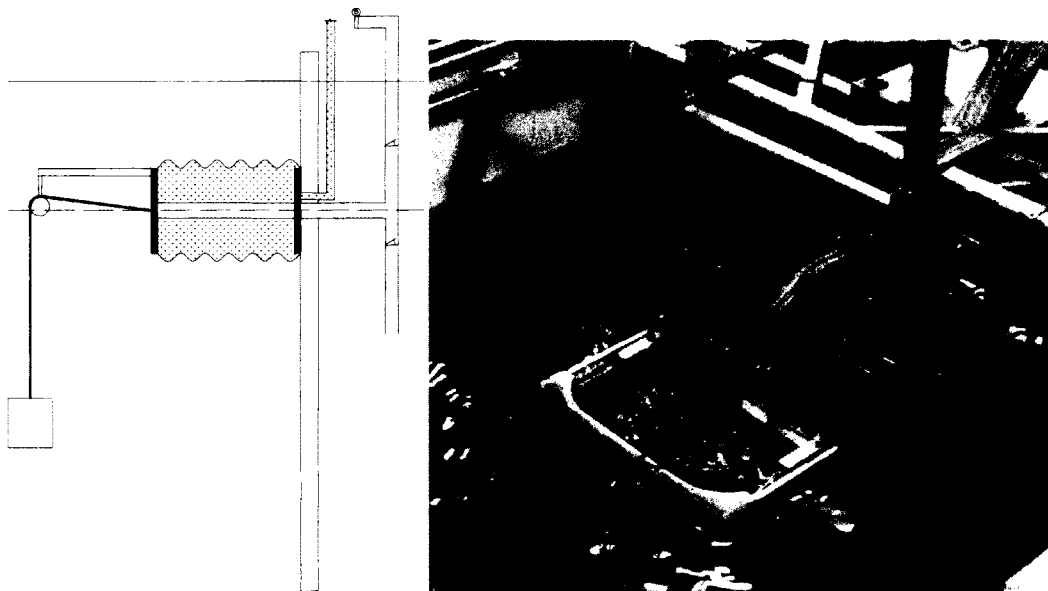


Figure 3.6 Horizontal Orientation

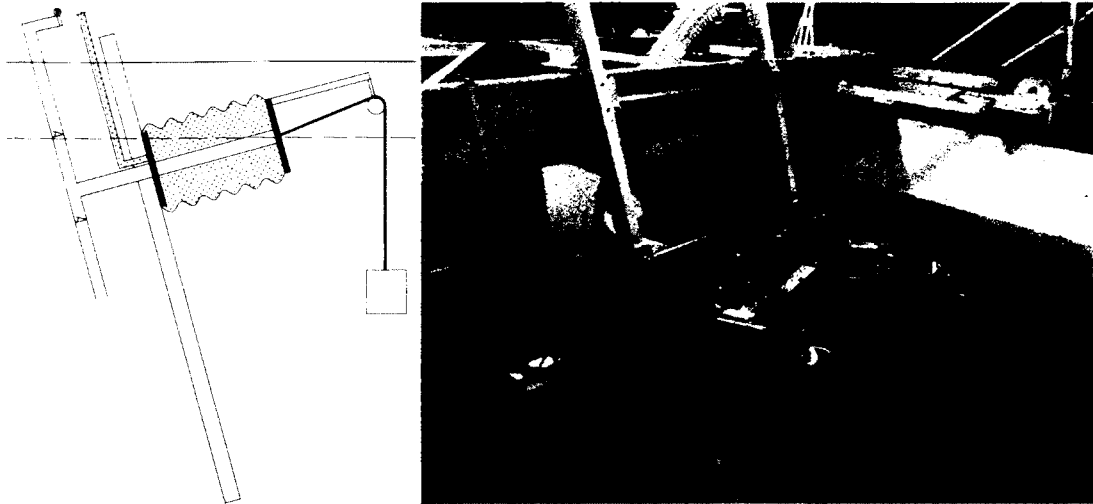


Figure 3.7 Upward Orientation

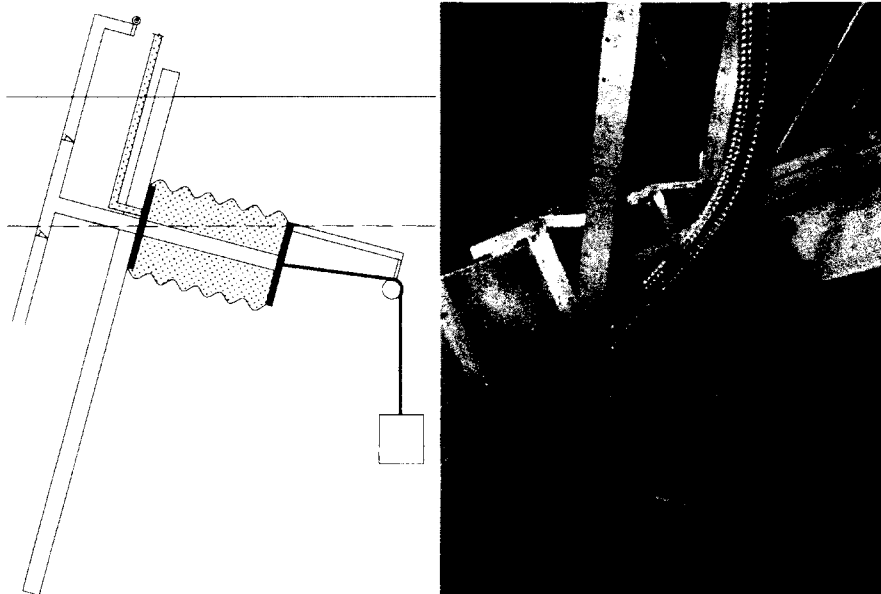


Figure 3.8 Downward Orientation

Preliminary testing results indicated that the SOWEC G-2 bellows worked well in both compression and expansion. No leakage issue occurred. The restoring force weights were found to be sufficient.

3.6 Testing Plan

Three combinations of wave heights and periods were tested on the SOWEC G-2. For each wave period, maximum wave height was used, when possible. The SOWEC G-2 was also positioned at various depths and orientations. Depth ranged from the surface to 11 inches below the mean water level and the device was also placed perpendicular and angled to the progressing waves (± 35 degrees). In addition, experiments were performed with and without the previously described enhancement structures (kinetic control surface, extension plate and shoal plane). These configurations, load cases and bellows depth related in a total of 189 experiments. In all cases, the pump-type power take-off unit was employed. Flow exit height, pressure and flow rate were recorded so that output power could be calculated. The overall testing plan is shown in Table 3.2.

Table 3.2 Testing Configuration Plan

SOWEC G-2 Scale Model Test Plan				
Orientation	Bellows depth	Enhancements	Period	Wave height
	(inch)		$T_{(s)}$	$H_{(m)}$
HORIZONTAL	6	Kinetic control surface /Extension Plate /Shoal Plane	1.5	0.351
	4		2	0.281
	0		2.5	0.211
DOWNWARD	11		1.5	0.351
	9		2	0.287
	6		2.5	0.211
UPWARD	9		1.5	0.351
	7		2	0.287
	4		2.5	0.211

Bellows depth: The center of bellows pressure plate below water level

It should be noted, however, that it was quickly established that upward oriented tests yielded very low efficiencies and the device was vulnerable to damage. So upward oriented testing was curtailed prior to complete the full suite of planned experiments.

Chapter 4

Experiment Data Processing and Results

4.1 Efficiency Calculation

Power output efficiency was calculated for the experiments in which all data was recorded. Efficiency was calculated as the capture power divide the available wave power,

$$Z_c = W_{op} / W_e , \quad (4.1.1)$$

where Z_c is the efficiency, W_{op} is the captured power, and W_e is the wave power.

The captured power W_{op} is the product of the pressure and flow rate so that

$$W_{op} = P * Q , \quad (4.1.2)$$

where P is the pressure recorded from the visual pressure gauge, and Q is the volumetric flow rate, determined by measuring the rate of water pumped through the orifice into an open container. The flow rate Q is given by

$$Q = A * V , \quad (4.1.3)$$

where A is the orifice section area, and V is the flow velocity through the section area.

The average capture power was calculated using the peak pressure and the average pressure recorded during the experiments. These analysis procedure is described in more detail in section 4.1.1 and 4.1.2.

Wave power, W_e , is the product of wave energy flux and structure width,

$$W_e = \mathcal{F} * b , \quad (4.1.4)$$

where \mathcal{F} is wave energy flux, and b is the breadth of the device perpendicular to wave direction. The wave energy flux is the product of the total average energy per unit surface area of the wave and group velocity,

$$\mathcal{F} = E * C_g , \quad (4.1.5)$$

where E is the total average energy per unit surface area of the wave, and C_g is the group velocity. E is calculated as the sum of the potential and kinetic energy so that

$$E = \frac{\rho g H^2}{8} , \quad (4.1.6)$$

where ρ is density; g is gravitational acceleration, and H is wave height.

The group velocity, C_g , is the speed at which the energy is transmitted and is given by the following

$$C_g = \frac{C}{2} * \left(1 + \frac{2kh}{\sinh 2kh} \right), \quad (4.1.7)$$

and

$$C = \frac{\sigma}{k} , \quad (4.1.8)$$

where C is wave celerity, σ is radian frequency (see Eqn 2.5.6) and k is wave number (see Eqn 2.5.4).

4.1.1 Peak Pressure Method for Determining Output Power.

This method of calculating the output power assumes that the device generates peak pressure continuously, and uses the visual pressure gauge peak pressure reading for the calculation. Since the visual pressure gauge recording was 2.34 meters above pump level, the piston water pump pressure P is

$$P = P_1 + \rho g \Delta h, \quad (4.1.9)$$

where Δh is the height above the pump to pressure gauge, and P_1 is the visual pressure gauge reading. The average volume rate of flow was used for Q , and was measured as the discharge volume over several wave cycles per corresponding time interval. The peak pressure power, wave power and efficiency were calculated using Equation 4.1.2, 4.1.4 and 4.1.1

Eighteen groups of data for which the peak pressure efficiency exceeded 30% were chosen for inclusion in Table 4.1. (All results are provided in Appendix A.) Wave periods include 1.5s, 2s, 2.2 s, and 2.5s. Enhancements included kinetic control surface (KCS), extension plate (EP) and shoal plane (SP). Results indicated that the output power increased when submerged depth increased from 0.108m to 0.203m. The maximum output power was obtained for a 1.5 second wave period, 0.351m wave height, and depth of 0.203m.

SOWEC G-2 Peak Power Efficiency Results

Frame Direction	Depth	Period	Wave Height	Enhancements	Wave Length	Wave Power	Peak Pressure	Flow Rate	Peak Capture Power	Peak Efficiency	Ob NO.	Date
	D, (m)	T, (s)	H, (m)		L, (m)	We,(watt)	P, (psi)	Q, (GPM)	Wop, (watt)	Zc	#	
HORIZONTAL	-0.108	1.5	0.351	KCS	3.514	134.163	19.0	4.983	48.580	36.21%	57	17-Jun
HORIZONTAL	-0.108	1.5	0.351	KCS+EP	3.514	134.163	15.0	5.606	44.893	33.46%	101	1-Jul
HORIZONTAL	-0.133	2	0.287	KCS+EP	6.163	125.764	16.5	4.376	37.895	30.13%	133	28-Jul
HORIZONTAL	-0.133	1.5	0.351	KCS+EP	3.514	134.163	19.5	5.276	52.586	39.20%	134	28-Jul
HORIZONTAL	-0.133	1.5	0.351	KCS+EP	3.514	134.163	14.7	5.606	44.161	32.92%	137	28-Jul
DOWNWARD	-0.203	1.5	0.351	KCS+EP	3.514	134.163	18.5	5.276	50.289	37.48%	140	28-Jul
DOWNWARD	-0.203	1.5	0.351	KCS+EP	3.514	134.163	17.5	4.983	45.327	33.78%	143	28-Jul
DOWNWARD	-0.203	1.5	0.351	KCS+EP	3.514	134.163	13.8	5.606	41.965	31.28%	149	28-Jul
DOWNWARD	-0.203	1.5	0.351	KCS+EP	3.514	134.163	19.0	5.606	54.652	40.74%	152	28-Jul
HORIZONTAL	-0.165	1.5	0.351	KCS	3.514	134.163	18.2	5.276	49.601	36.97%	164	3-Aug
DOWNWARD	-0.203	1.5	0.351	KCS	3.514	134.163	15.0	5.276	42.252	31.49%	167	3-Aug
DOWNWARD	-0.203	1.5	0.351	KCS	3.514	134.163	14.8	5.126	40.599	30.26%	170	3-Aug
HORIZONTAL	-0.133	1.5	0.351	KCS	3.514	134.163	16.5	4.849	41.992	31.30%	181	3-Aug
HORIZONTAL	-0.133	2.2	0.254	KCS+EP+SL	7.329	112.365	26.0	2.848	36.435	32.43%	198	16-Aug
DOWWARD	-0.229	2.2	0.254	KCS+EP+SL	7.329	112.365	31.0	3.041	45.522	40.51%	201	16-Aug
HORIZONTAL	-0.191	2.2	0.254	KCS+EP+SL	7.329	112.365	25.0	3.204	39.595	35.24%	205	17-Aug
HORIZONTAL	-0.191	2.2	0.254	KCS+EP+SL	7.329	112.365	22.5	3.385	38.154	33.95%	207	17-Aug
HORIZONTAL	-0.191	2	0.287	KCS+EP+SL	6.163	125.764	25.0	3.518	43.477	34.57%	208	17-Aug
DOWNWARD	-0.203	2.5	0.211	KCS+EP+SL	9.107	92.692	23.0	3.093	35.538	38.34%	209	17-Aug
DOWNWARD	-0.203	2.2	0.254	KCS+EP+SL	7.329	112.365	26.5	3.385	44.046	39.20%	210	17-Aug
DOWNWARD	-0.203	2.2	0.254	KCS+EP+SL	7.329	112.365	31.5	3.093	46.980	41.81%	212	17-Aug
DOWNWARD	-0.203	2.2	0.254	KCS+EP+SL	7.329	112.365	22.5	3.588	40.443	35.99%	216	17-Aug

Table 4.1 Peak Power Efficiency Results

4.1.2 Average Pressure Times Flow Rate Method for Determining Output Power

This method of calculating the output power of the device assumes that the pressure fluctuation was sinusoidal and flow rate can be computed by using an orifice coefficient approach. The coefficient was obtained by matching observed measured discharge rates. The time average of the product of pressure and flow rate was then used to calculate average power output.

The pressure was assumed to oscillate smoothly in each wave period (Fig 4.1) between the maximum pressure and minimum pressure recorded by the visual pressure gauge. The instantaneous pressure was taken as

$$P_1 = P_{ave} + a \cos(\sigma t) , \quad (4.1.10)$$

where P_1 is the instantaneous pressure measured by the gauge; P_{ave} is the average pressure; “a” is the pressure fluctuation amplitude, and σ is the radian frequency (2π /wave period).

The average pressure P_{ave} was calculated by averaging the sum of the maximum pressure and minimum pressure,

$$P_{ave} = (P_{max} + P_{min})/2 . \quad (4.1.11)$$

The pressure fluctuation amplitude “a” was calculated as the difference between maximum pressure and minimum pressure divided by two,

$$a = (P_{max} - P_{min})/2 . \quad (4.1.12)$$

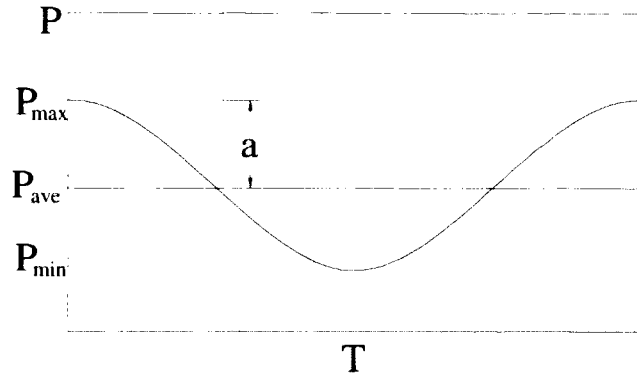


Fig 4.1 Pressure Fluctuation Graphical Definition

To obtain the flow rate, the conservation of energy approach was employed. Taking the flow to be steady-state, incompressible and inviscid in a horizontal pipe (Fig 4.2), without potential energy change, the Bernoulli equation can be used to related two points on the same streamline:

$$\frac{P_1}{\rho} + \frac{V_1^2}{2} = \frac{P_2}{\rho} + \frac{V_2^2}{2} \quad , \quad (4.1.13)$$

where P_1 is the pressure upstream from orifice, and P_2 is the downstream pressure which will flow out directly. V_1 is the flow velocity from the piston water pump, and V_2 is the output flow velocity. This method assumes that the flowing fluid is incompressible even though pressure varies. The density was assumed to remain approximately constant.

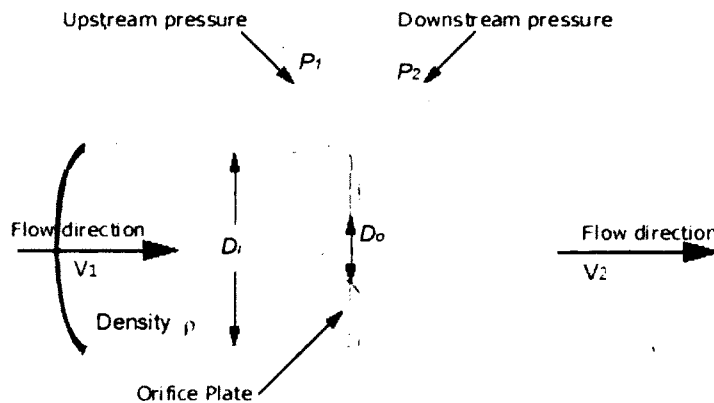


Fig 4.2 Flow Through the Orifice Inside the Pipe

In Figure 4.2, D_i is the diameter of the horizontal upstream pipe, and D_o is the diameter of the orifice plate. Various diameter orifice plates were used in the testing. Diameters include 0.1875 inch, 0.2187 inch, 0.25 inch, 0.3125 inch. The smaller diameter orifices generated the larger efficiency values as shown in the test results (Table 4.1).

Applying Equation 4.1.13 between D_i and D_o neglecting losses, and setting P_2 equal to zero at the downstream zone, the volumetric flow rate can be expressed as

$$Q = \left[\frac{A_i^2 A_o^2}{A_i^2 - A_o^2} \right]^{1/2} \sqrt{2P_1/\rho} , \quad (4.1.14)$$

where A_i is the section area of the pipe, and A_o is the section area of the orifice. The volumetric flow rate Q obeys the continuity equation on both sides of the orifice plate.

Incorporating losses using a discharge coefficient C_o , the equation of flow rate can be written as

$$Q = C_o \left[\frac{A_i^2 A_o^2}{A_i^2 - A_o^2} \right]^{1/2} \sqrt{2P_1/\rho} . \quad (4.1.15)$$

The discharge coefficient C_o was calculated by time averaging over one cycle:

$$C_o = \frac{Q_{ave} T}{\left[\frac{2A_i^2 A_o^2}{\rho(A_i^2 - A_o^2)} \right]^{1/2} \int_0^T (P_{ave} + a \cos \sigma t)^{1/2} dt} , \quad (4.1.16)$$

where Q_{ave} is the average flow rate measured as the discharge volume over several wave cycles divided by the corresponding time interval.

Since P_1 is the pressure measured 2.34 meters above the pump, the piston water pump pressure P is

$$P = P_1 + \rho g \Delta h, \quad (4.1.17)$$

where Δh is the height above the pump to the pressure gauge, and P_1 is given by Equation 4.1.10.

The average output power W_{oa} was calculated by time averaging over one cycle:

$$W_{oa} = \frac{1}{T} \int_0^T P Q dt . \quad (4.1.18)$$

Substituting Equation 4.1.10, 4.1.15 and 4.1.17 yields

$$W_{oa} = \frac{C_o}{T} \left[\frac{2A_i^2 A_o^2}{\rho(A_i^2 - A_o^2)} \right]^{\frac{1}{2}} \int_0^T (P_{ave} + a \cos \sigma t + \rho g \Delta h) (P_{ave} + a \cos \sigma t)^{1/2} dt \quad (4.1.19)$$

Eighteen groups of data for which the average pressure efficiency exceeded 20% were chosen in for inclusion Table 4.2. (All results are provided in Appendix A.) Wave periods include 1.5s, 2s, 2.2 s, and 2.5s. Enhancements include kinetic control surface (KCS), extension plate (EP) and shoal plane (SP). Results indicate that the output power increased when submerged depth increased from 0.108m to 0.203m. The maximum output power was obtained for a 1.5 second wave period, 0.351m wave height, and depth of 0.203m. It should be noted that efficiencies calculated using this method were about 25% less than those obtained using the peak pressure method.

Table 4.2 Average Power Efficiency Results

SOWEC G-2 Average Power Efficiency Results														
Frame Direction	Depth	Period	Wave Height	Enhancements	Orifice Diameter	Wave Length	Wave Power	Flow Rate	Average Pressure	Discharge Coefficient	Average Capture Power	Average Efficiency	Ob NO	Date
unit	D, (m)	T, (s)	H, (m)		Do, (in)	L, (m)	We, (watt)	Q, (GPM)	Pave, (psi)	Co	Woa, (watt)	Zc	#	
HORIZONTAL	-0.108	1.5	0.351	KCS	0.250	3.514	134.163	4.993	13.50	0.141	36.069	26.88%	57	17-Jun
HORIZONTAL	-0.108	1.5	0.351	KCS+EP	0.313	3.514	134.163	5.617	9.50	0.153	31.947	23.81%	101	1-Jul
HORIZONTAL	-0.133	2	0.287	KCS+EP	0.250	6.163	125.764	4.384	11.00	0.138	27.412	21.80%	133	28-Jul
HORIZONTAL	-0.133	1.5	0.351	KCS+EP	0.250	3.514	134.163	5.287	13.60	0.149	38.598	28.77%	134	28-Jul
HORIZONTAL	-0.133	1.5	0.351	KCS+EP	0.313	3.514	134.163	5.617	9.35	0.154	31.519	23.49%	137	28-Jul
DOWNWARD	-0.203	1.5	0.351	KCS+EP	0.250	3.514	134.163	5.287	13.25	0.151	37.544	27.98%	140	28-Jul
DOWNWARD	-0.203	1.5	0.351	KCS+EP	0.250	3.514	134.163	4.993	12.75	0.145	34.253	25.53%	143	28-Jul
DOWNWARD	-0.203	1.5	0.351	KCS+EP	0.313	3.514	134.163	5.617	9.40	0.152	30.973	23.09%	149	28-Jul
DOWNWARD	-0.203	1.5	0.351	KCS+EP	0.250	3.514	134.163	5.617	13.50	0.159	40.578	30.25%	152	28-Jul
HORIZONTAL	-0.165	1.5	0.351	KCS	0.250	3.514	134.163	5.287	12.70	0.154	36.534	27.23%	164	3-Aug
DOWNWARD	-0.203	1.5	0.351	KCS	0.250	3.514	134.163	5.287	11.50	0.161	33.123	24.69%	167	3-Aug
DOWNWARD	-0.203	1.5	0.351	KCS	0.250	3.514	134.163	5.136	11.50	0.156	32.114	23.94%	170	3-Aug
HORIZONTAL	-0.133	1.5	0.351	KCS	0.250	3.514	134.163	4.858	11.75	0.147	31.409	23.41%	181	3-Aug
HORIZONTAL	-0.133	2.2	0.254	KCS+EP+SL	0.188	7.329	112.365	2.853	14.75	0.107	24.336	21.66%	198	16-Aug
DOWNWARD	-0.229	2.2	0.254	KCS+EP+SL	0.188	7.329	112.365	3.047	17.75	0.104	30.225	26.90%	201	16-Aug
HORIZONTAL	-0.191	2.2	0.254	KCS+EP+SL	0.188	7.329	112.365	3.210	14.40	0.121	26.585	23.66%	205	17-Aug
HORIZONTAL	-0.191	2.2	0.254	KCS+EP+SL	0.219	7.329	112.365	3.392	12.50	0.119	25.588	22.77%	207	17-Aug
HORIZONTAL	-0.191	2	0.287	KCS+EP+SL	0.219	6.163	125.764	3.525	14.00	0.116	29.035	23.09%	208	17-Aug
DOWNWARD	-0.203	2.5	0.211	KCS+EP+SL	0.219	9.107	92.692	3.099	12.50	0.109	23.757	25.63%	209	17-Aug
DOWNWARD	-0.203	2.2	0.254	KCS+EP+SL	0.219	7.329	112.365	3.392	14.50	0.111	29.248	26.03%	210	17-Aug
DOWNWARD	-0.203	2.2	0.254	KCS+EP+SL	0.188	7.329	112.365	3.099	18.35	0.103	31.304	27.86%	212	17-Aug
DOWNWARD	-0.203	2.2	0.254	KCS+EP+SL	0.250	7.329	112.365	3.595	12.35	0.111	27.089	24.11%	216	17-Aug

4.1.3 Comparison of the Output Power and Estimated Power

The peak power and average power were used as comparative assessments of the SOWEC G-2 output power. Peak power, average power, full ellipse stroke estimated power and bellows full stroke estimated power are compared in Table 4.3.

In Table 4.3, z is the center position of the bellow submerged depth at each depth, the device was tested under three wave conditions (1.5 second wave with 0.351m wave height, 2 second wave with 0.287m wave height, 2.5 second wave with 0.211m wave height). The bellows full stroke estimated power values are greater than the full ellipse stroke estimated power values, and peak power results are greater than average power values. Both methods of estimating power yield results which are generally greater than the measured output power, but the full ellipse stroke estimated power is much closer. For example, for the testing #1, the full ellipse stroke estimated power was about 100% larger than the peak pressure power, whereas the bellows full stroke estimated power was about 250% larger.

Table 4.3 Comparison of Estimated Power and Measured Output Power

Comparison of Estimated Power and Measured Output Power										
Depth	Period	Wave Length	Wave Height	Ellipse Length	Bellows Distance	Force	Estimate Ellipse Power	Estimate Bellows Power	Peak Capture Power	Average Capture Power
z , (m)	T, (s)	L, (m)	H, (m)	ρ_{max} , (m)	δ_b , (m)	F, (N)	Wp, (watt)	Wb, (watt)	Wop, (watt)	Woa, (watt)
-0.108	1.5	3.514	0.351	0.145	0.229	408.832	78.906	124.83	35.691	24.796
-0.108	2	6.163	0.287	0.131	0.229	363.792	47.497	83.308	14	10.787
-0.108	2.5	9.107	0.211	0.106	0.229	278.160	23.479	50.959	N/A	N/A
-0.133	1.5	3.514	0.351	0.138	0.229	390.689	72.058	119.29	26.413	19.750
-0.133	2	6.163	0.287	0.127	0.229	354.654	45.141	81.216	22.371	16.609
-0.133	2.5	9.107	0.211	0.104	0.229	273.704	22.733	50.143	11.337	8.698
-0.165	1.5	3.514	0.351	0.131	0.229	369.139	64.328	112.71	49.6	36.534
-0.165	2	6.163	0.287	0.123	0.229	343.565	42.362	78.676	34.658	25.141
-0.165	2.5	9.107	0.211	0.102	0.229	268.253	21.836	49.144	15.615	11.889
-0.191	1.5	3.514	0.351	0.125	0.229	352.759	58.745	107.709	52.586	38.598
-0.191	2	6.163	0.287	0.120	0.229	334.953	40.265	76.704	43.477	29.035
-0.191	2.5	9.107	0.211	0.100	0.229	263.984	21.147	48.362	23.666	16.176
-0.203	1.5	3.514	0.351	0.122	0.229	344.844	56.139	105.292	54.652	40.578
-0.203	2	6.163	0.287	0.119	0.229	330.732	39.257	75.738	34.939	25.554
-0.203	2.5	9.107	0.211	0.099	0.229	261.880	20.811	47.977	13.297	10.325
-0.229	1.5	3.514	0.351	0.117	0.229	329.543	51.268	100.62	35.75	27.000
-0.229	2	6.163	0.287	0.116	0.229	322.456	37.317	73.842	28.87	20.924
-0.229	2.5	9.107	0.211	0.098	0.229	257.733	20.157	47.217	8.796	6.773

4.2 Experimental Data Analysis and Evaluation

To supply useful information for future full scale device design and to evaluate device performance, efficiency results were examined. In particular, the relationships between efficiency and depth, orientation, wave period and enhancements were explored.

For the efficiency vs. depth comparison (Fig 4.3), the blue line indicates peak pressure efficiency, and the red line indicates average pressure efficiency. Average pressure efficiency was 8.58% when the center of bellows pressure plate was even with the mean water level. Efficiency increased to 21.80% when the bellows was submerged 4 inches, but dropped down to 16.18% when the bellows center was submerged to 6 inches below water level. Peak pressure efficiency was 11.13% when the center of bellows pressure plate was at the mean water level. Efficiency increased to 30.13% when the bellows was submerged 4 inches, but dropped down to 22.50% when bellows was submerged to 6 inches below water level.

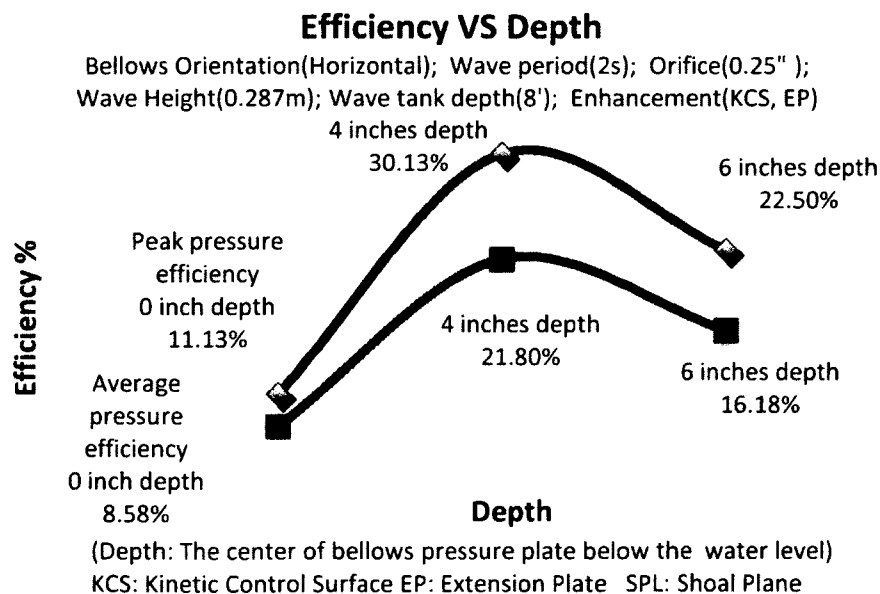


Fig 4.3 Efficiency VS Depth

For the efficiency vs. orientation comparison (Fig 4.5), the blue line indicates peak pressure efficiency, and the red line indicates average pressure efficiency. Average pressure efficiency increased from 2.62% to 8.57% when the bellows orientation changed from upward to horizontal, and ultimately reached 20.31% for the downward orientation. Peak pressure efficiency increased from 3.17% to 11.13% when the bellows orientation changed from upward to horizontal, and ultimately reached 27.78% in the downward orientation.

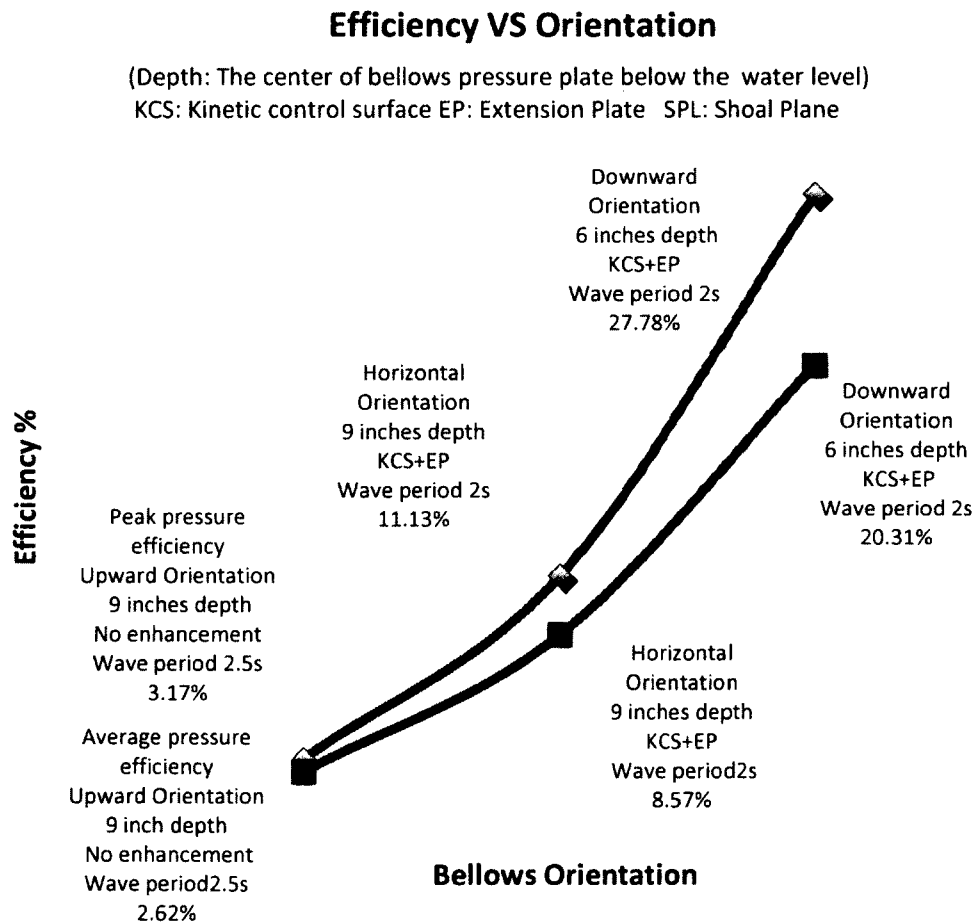


Fig 4.4 Efficiency VS Orientation

For the efficiency vs. slope angle comparison (Fig 4.4), the blue line indicates peak pressure efficiency, and the red line indicates average pressure efficiency. Average pressure efficiency increased from 16.64% to 19.41% when the bellows downward slope angle decreased from 35 degrees to 15 degrees. Peak pressure efficiency increased from 22.96% to 27% when the bellows downward slope angle decreased from 35 degrees to 15 degrees.

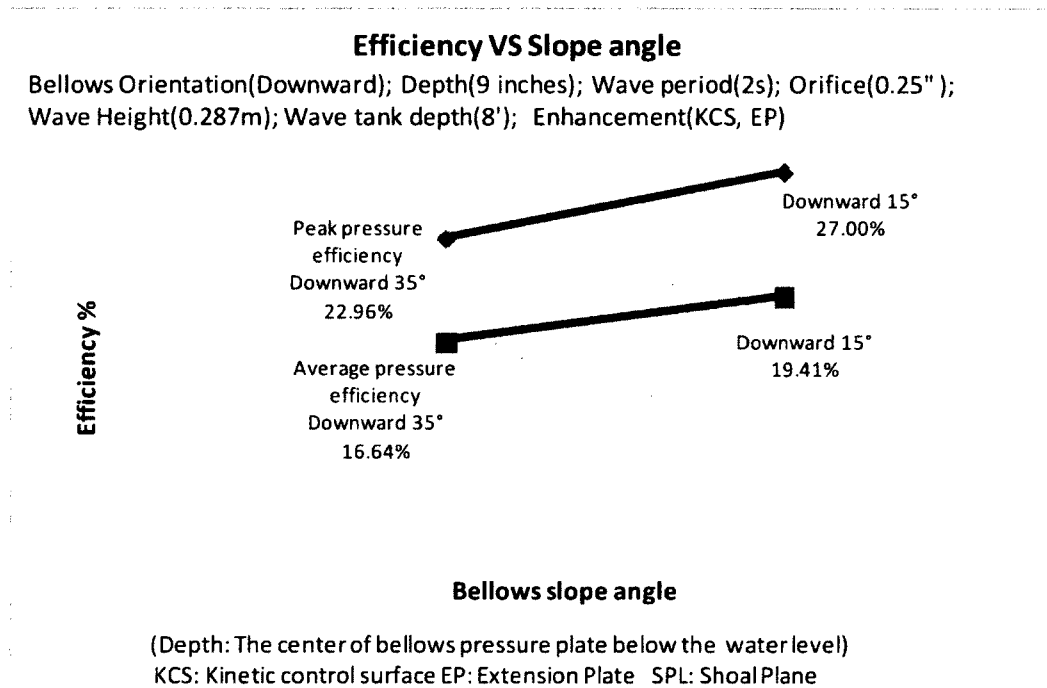


Fig 4.5 Efficiency VS Downward Slope Angle

For the efficiency vs. wave period comparison (Fig 4.6), the blue line indicates peak pressure efficiency, and the red line indicates average pressure efficiency. Average pressure efficiency increased from 13.50% to 20.18% when the wave period changed from 2.5s to 2.0s, and ultimately reached 28.77% for the 1.5s wave. Peak pressure efficiency increased from 17.42% to 30.13% when the wave period changed from 2.5s to 2.0s, and ultimately reached 39.2% for the 1.5s wave.

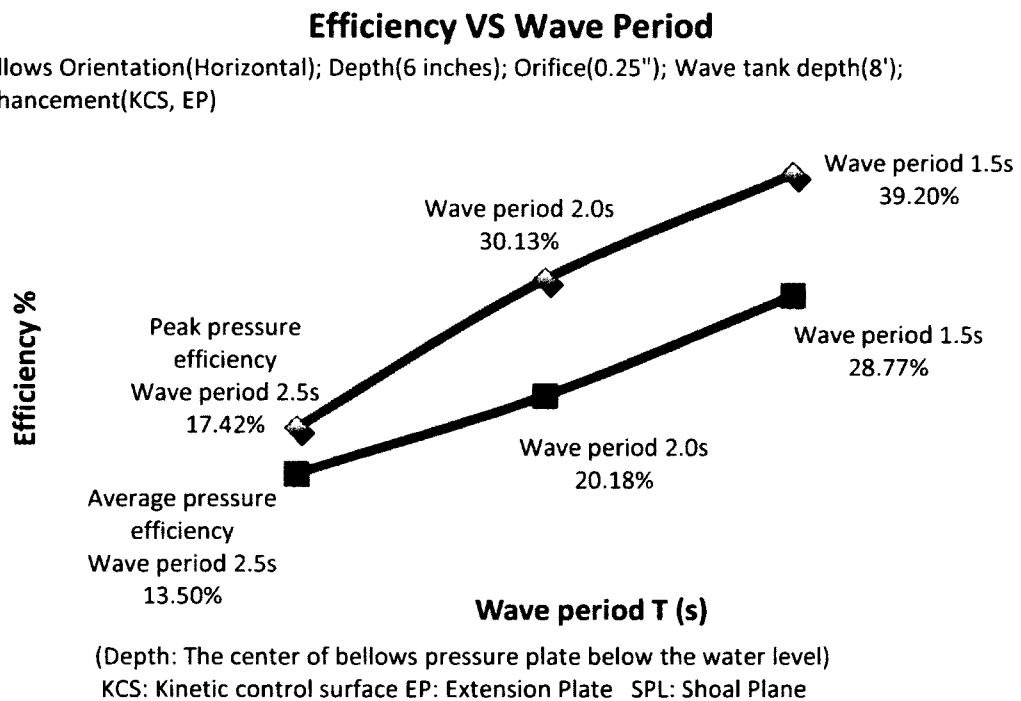


Fig 4.6 Efficiency VS Wave Period

For the efficiency vs. enhancement comparison (Fig 4.7), the blue line indicates peak pressure efficiency, and the red line indicates average pressure efficiency. Average pressure efficiency increased from 18.06% to 20.32% when the extension plate was added to kinetic control surface, and ultimately reached 21.69% with all enhancements. Peak pressure efficiency increased from 23.06% to 27.78% when the extension plate was added to kinetic control surface, and ultimately reached 28.62% with all enhancements.

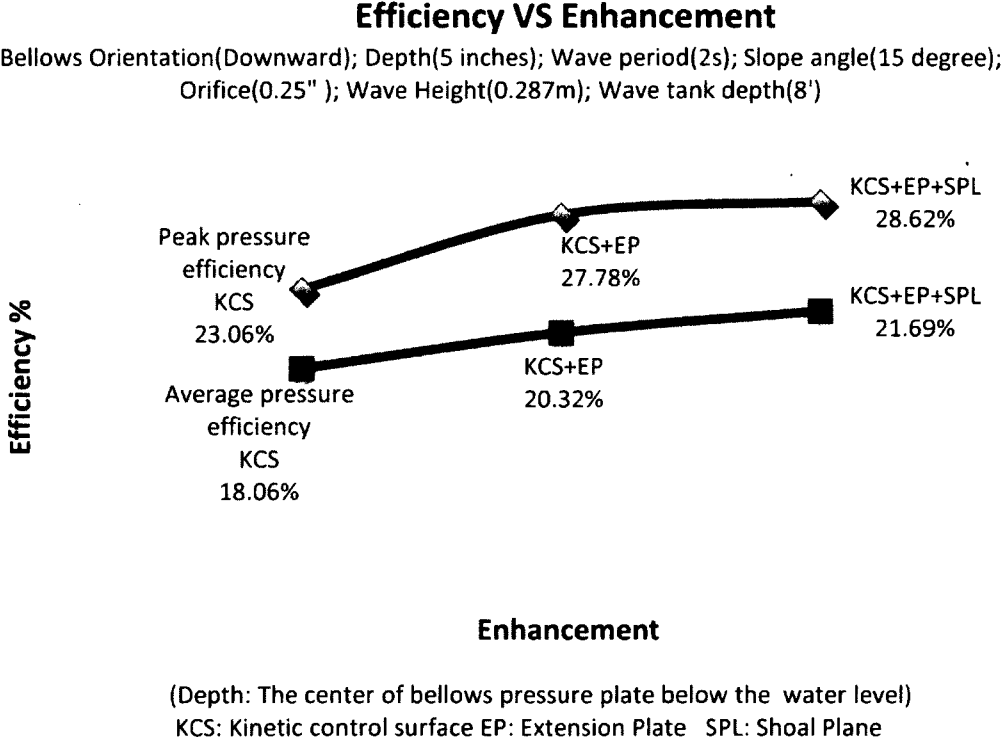


Fig 4.7 Efficiency VS Enhancement

The highest efficiency occurred when the bellows was orientated 15 degrees downward, the center of the bellows pressure plate was 6 inches below water level, the kinetic control surface and extension plate were added, wave period was 1.5 second, and wave height was 0.351 meters. Under these conditions, peak pressure efficiency was 40.74%, and average pressure efficiency was 30.25%.

4.3 Experimental Input Power Calculation

During wave experiments, time series for surface elevation and pressure plate displacement were obtained using OPIE (Michelin, D., Stott, S.1997). Assuming a simple mathematical form for the observed time series and predicting wave pressure on the plate using linear wave theory, the average power applied to the device due to wave pressure could be inferred. This may be regarded as a basic standard for the potential power the device could produce.

The bellows pressure plate displacement and surface elevation were monitored and recorded by the OPIE system (Fig 4.8).

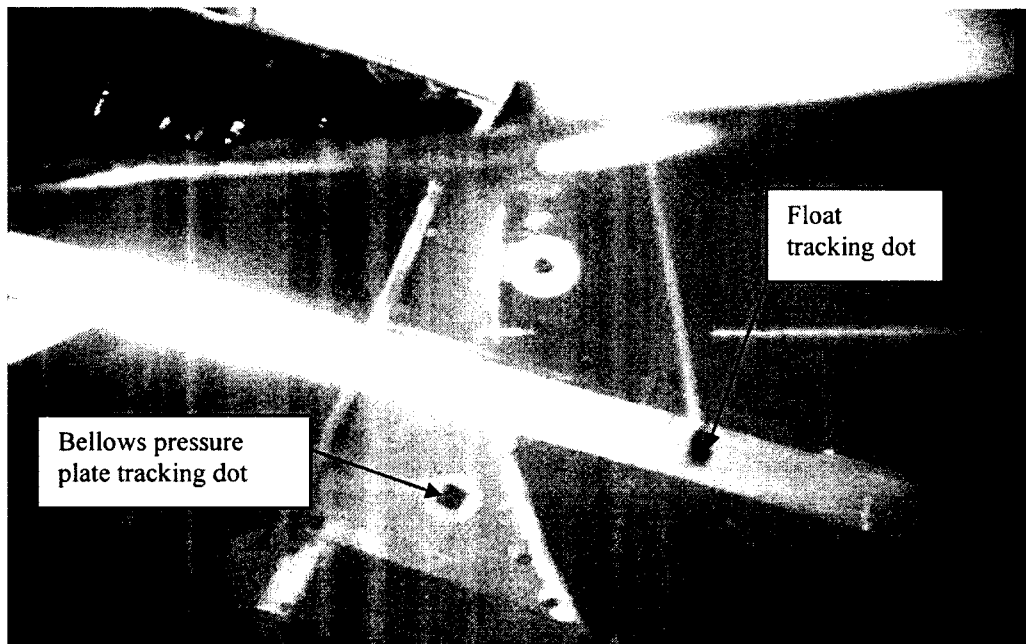


Fig 4.8 OPIE Tracking System

A typical time series is shown in Fig 4.9. These curves were approximated using an appropriate sine wave having the same amplitude, period and relative phase relationship.

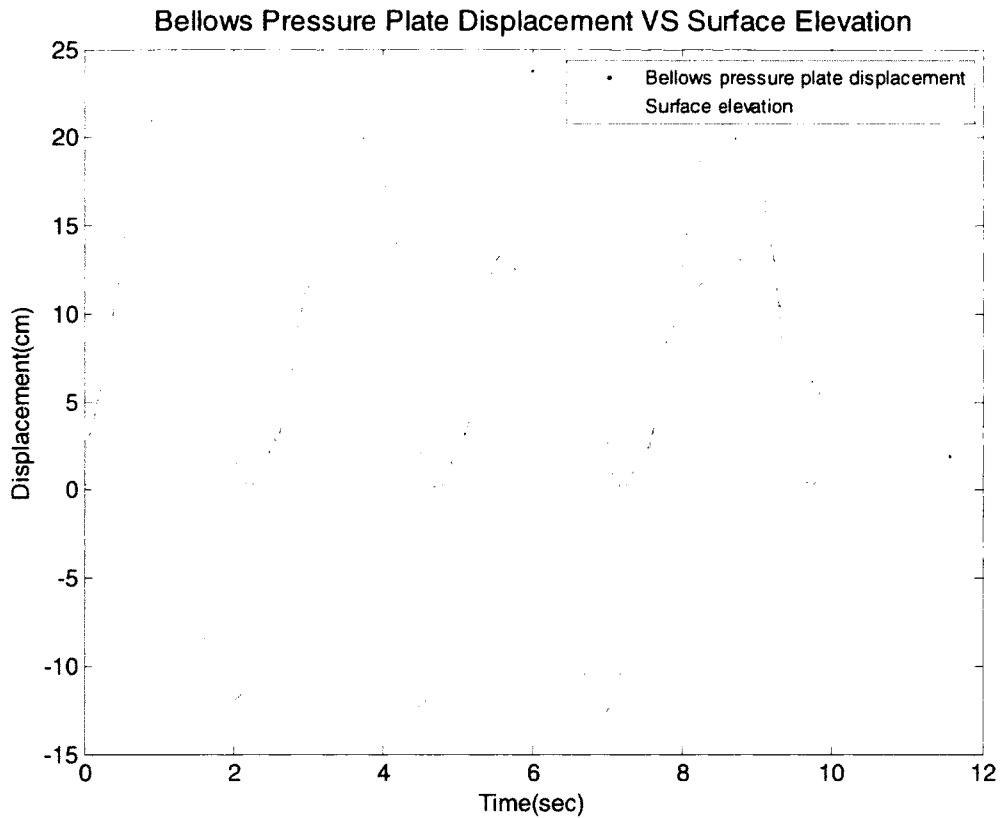


Fig 4.9 Bellows Pressure Plate Displacement VS. Surface Elevation (Aug 08 #04 test)

Surface elevation η is modeled as a sine wave,

$$\eta = a \sin \omega t , \quad (4.3.1)$$

where “a” is the surface elevation amplitude.

Pressure plate displacement, x , the distance the bellows pressure plate moves inward relative to its fully expanded position, is modeled according to

$$x = A - A \cos \omega t , \quad (4.3.2)$$

where A is half of the bellows pressure plate horizontal stroke displacement.

These mathematical representations are plotted in Fig 4.10

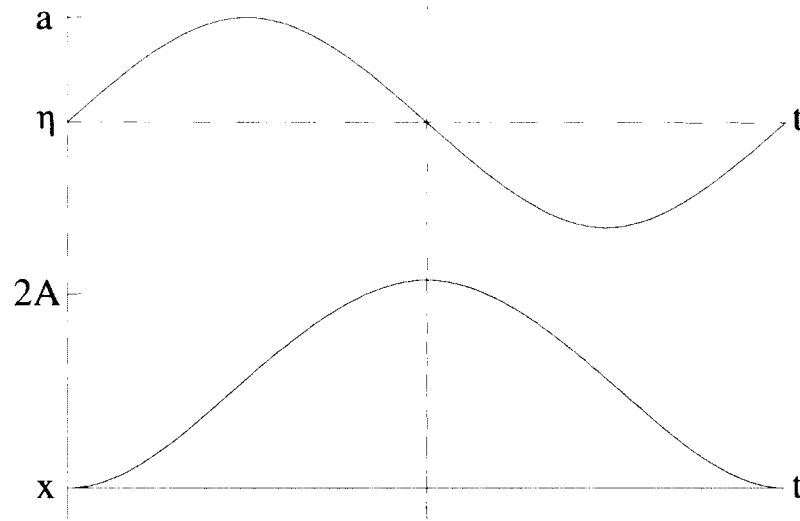


Fig 4.10 Surface Elevation and Bellows Pressure Plate Horizontal Displacement
Mathematical Model.

The power applied to the device by wave pressure can be calculated by

$$W_p = F \left(\frac{dx}{dt} \right). \quad (4.3.3)$$

where F is the force on the pressure plate due to wave pressure and x is the displacement of the pressure plate in the compression direction from its fully expanded position.

The average power over a wave cycle applied to the device is then

$$W_a = \frac{1}{T} * \int_0^{T/2} F * \left(\frac{dx}{dt} \right) dt , \quad (4.3.4)$$

where T is wave period. Substituting

$$F = \rho * g * \eta * K_p * A_p , \quad (4.3.5)$$

η from Eqn 4.3.1, x from Eqn 4.3.2, and K_p from Eqn 2.5.3, and completing the integral, average power becomes

$$W_a = \frac{A_p}{2} \rho g a A \sigma K_p \quad (4.3.6)$$

This equation is applied to the three experiments shown in Fig 4.9, 4.11 and 4.12.

For test #4 done on Aug 08, 2011, (Fig 4.9), the average power applied to the plate by wave pressure calculated from Equation 4.3.6 was 53.67 W. For this test, the wave period was 2.5 seconds; the wave height was 0.211 meters; the bellows orientation was downward, and the center of the bellows pressure plate was 0.108 meters below the water level. For comparison, wave transport power was 92.69 W, and device average pressure power was 16.14 W.

For test #22 done on Aug 08, 2011, (Fig 4.11), the average power applied to the plate by wave pressure calculated from Equation 4.3.6 was 48.95 W. For this test, the wave period was 2.5 seconds; the wave height was 0.211 meters; the bellows orientation was downward, and the center of the bellows pressure plate was 0.108 meters below the water level. For comparison, wave transport power was 92.69 W, and device average pressure power was 10.68 W.

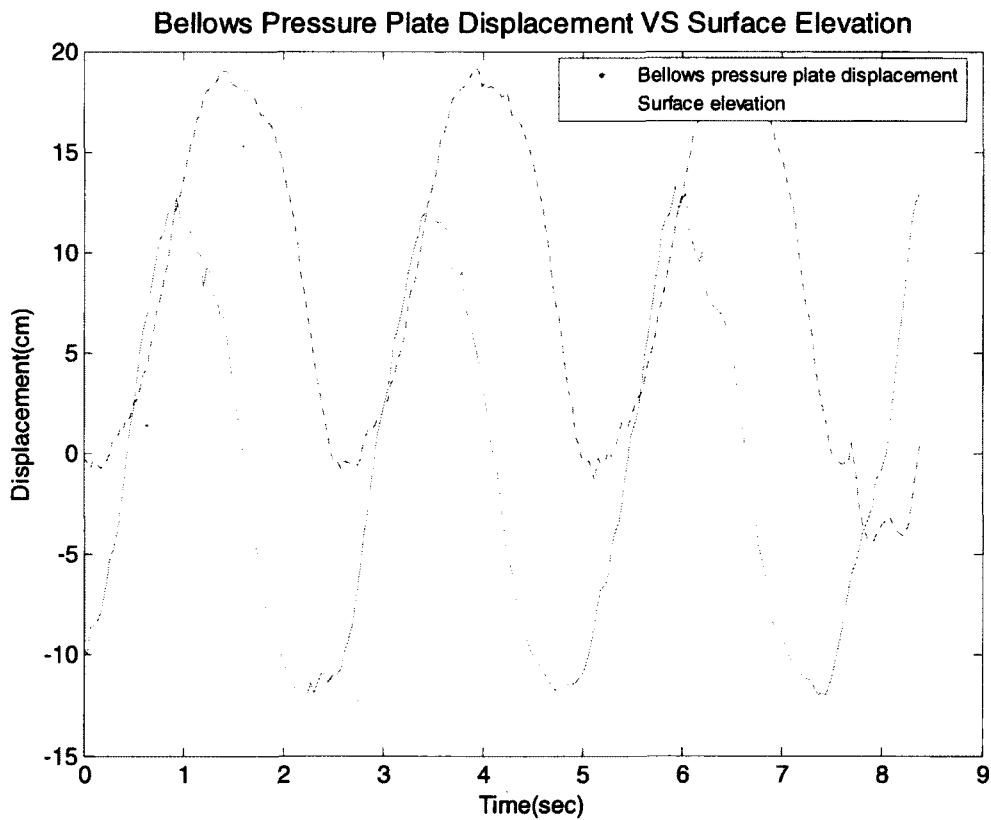


Fig 4.11 Bellows Pressure Plate Displacement VS. Surface Elevation (Aug 08 #22 test)

For test #3 done on Aug 16, 2011, (Fig 4.12), the average power applied to the plate by wave pressure calculated from Equation 4.3.6 was 34.88 W. For this test, the wave period was 2.5 seconds; the wave height was 0.211 meters; the bellows orientation was downward, and the center of the bellows pressure plate was 0.165 meters below the water level. For comparison, wave transport power was 92.69 W, and device average pressure power was 11.55 W.

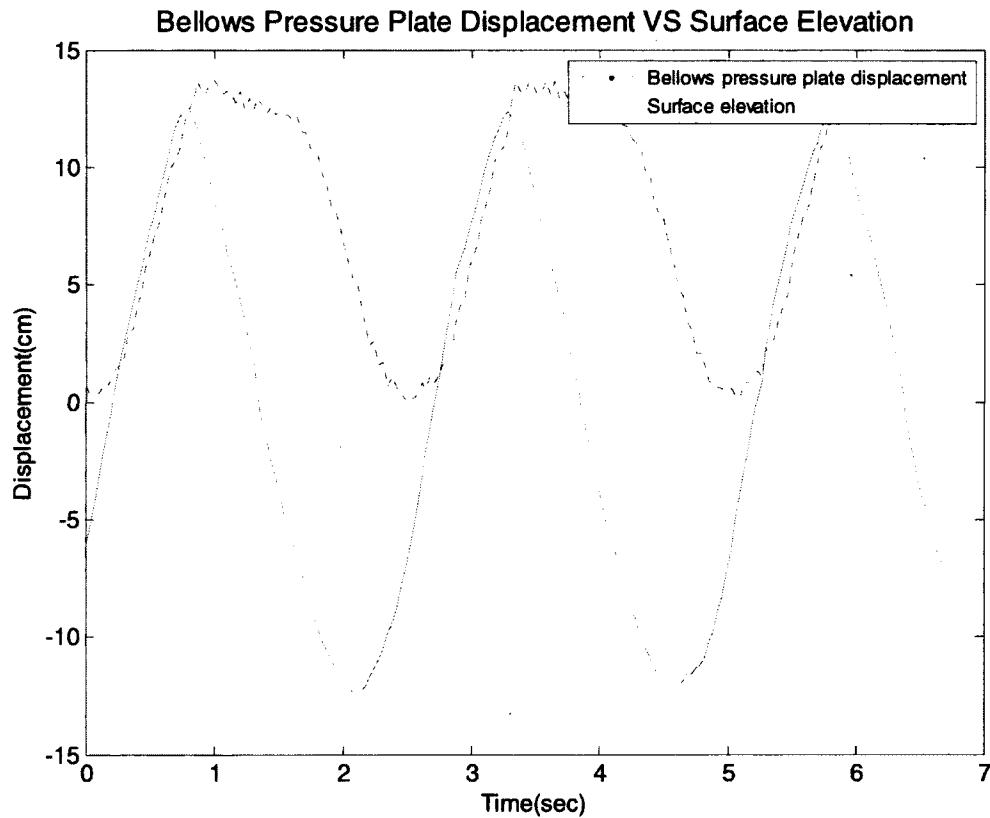


Fig 4.12 Bellows Pressure Plate Displacement VS. Surface Elevation (Aug 16 #03 test)

The wave power applied to the pressure plate was found to be about 3-5 times the device's output power measured from output pressure and flow rate. The power loss could be caused by bellows internal or external mechanism issues, as well as power take-off system.

4.4 Full Scale Power Prediction Using Froude Scaling

With the initial analysis complete, a full scale SOWEC-G2 was considered whose design replicated the 1/8th scale model tested. The full scale prototype is 288 inches long by 144 inches wide, and 120 inches high. A scaling ratio $L_r = L_{\text{proto}} / L_{\text{model}}$ of 8:1 was used. Froude scaling was chosen based on the fact that both inertial and gravitational forces play a major role in the wave and SOWEC-G2 dynamics. Therefore scaling was centered on keeping the Froude number constant between model and prototype,

$$(Fr)_p = (Fr)_m, \quad (4.4.1)$$

where $(Fr)_p$ is the Froude number of prototype, $(Fr)_m$ is the Froude number of scale model.

The Froude number is the square root of the ratio of inertial forces to gravitational forces and is given by

$$Fr = \frac{V}{\sqrt{gL}}, \quad (4.4.2)$$

where V = velocity, g = acceleration due to gravity, L is characteristic length. Combining yields $V_p/V_m = (L_r)^{1/2}$, $T_p/T_m = (L_r)^{1/2}$, and for similar densities $F_p/F_m = (L_r)^3$.

Full scale wave conditions, obtained by Froude scaling are given in Table 4.4.

Table 4.4 Open Ocean Wave Conditions Prediction.

Scale wave period prediction(T)			Scale wave height prediction(H)		
Period (s)	Model	Prototype	Wave height (m)	Model	Prototype
	1.50	4.74		0.35	2.81
	2.00	6.32		0.29	2.30
	2.50	7.91		0.21	1.69

The device power output is dimensionally the product of wave force (F) and device stroke displacement (L) divided by the wave period (T),

$$[W]_{\text{dim}} = FL/T \quad (4.4.3)$$

where $[W]_{\text{dim}}$ is power.

The ratio of prototype (full scale) output power to model measured output power is then

$$[W]_p / [W]_m = (L_r)^{7/2} , \quad (4.4.4)$$

so that
$$[W]_p = [W]_m (L_r)^{7/2} . \quad (4.4.5)$$

The optimal testing results indicated that the scale model peak pressure power was 54.65 W, and the average pressure power was 40.58 W. The prototype power, predicted from Equation 4.4.5, results in prototype peak pressure power of 79 kW, and average pressure power of 59 kW.

4.5 Performance Improvement Analysis

Performance improvement analysis is important to understanding SOWEC G-2 inefficiencies and to solve problems in future testing or full scale design. Due to several model scale characteristics limiting performance, energy losses occurred not only in the transmission of wave energy to the SOWEC G-2, and internally affecting output power. Energy losses could include stroke limitation loss, piston water pump loss, PTO pressure loss, restoring force loss, and enhancement structures loss.

4.5.1 Stroke Limitation

The bellows had a 22 cm maximum stroke displacement which restricted bellows compression. The bellows pressure plate hit the mechanical stops when wave amplitudes exceeded the bellows stroke limitation. This restriction created energy losses limiting wave power transport into the device.

4.5.2 Piston Water Pump

The low pressure piston water pump power take-off (PTO) was fabricated out of stainless steel pipe, a rubber piston and one-way valves. Energy loss could have occurred when the input power was transferred into output power due to high friction and hydraulic losses. Moreover, the rubber piston and one-way valves could also have leaked reducing the output pressure.

4.5.3 PTO Pressure

In this testing, the PTO pipe released flow directly to the atmosphere through fixed orifice. As a result, the output pressure oscillated over the wave cycle. If a variable load valve and container had been used, the output flow could have been accumulated and the output power would have been steadier.

4.5.4 Restoring Force

A constant weight block was applied as the restoring force system in this testing. When the wave force was less than the constant weight block, the bellows was not compressed. When the wave force was greater than the constant weight, the bellows was fully compressed but re-expansion was not completely finished. It would have been better if the bellows restoring force was variable over the wave period. This issue should be addressed using a variable restoring force system.

4.5.5 Enhancement Structures

Although the enhancement structures increased the efficiency in most of the testing, aspects of the enhancement structure could also decrease efficiency. For instance, the kinetic control surface and extension plate were made of stainless steel which increased the structure weight. When the structure became heavier, it consumed more wave energy to compress the bellows. Moreover, the shape of the shoal plane structure needed more investigation to increase efficiency.

CHAPTER 5

Conclusion

5.1 Discussion of Results

Wave tank testing was shown to be an efficient means for developing a wave energy design concept, as well as evaluating variations of the basic design. Scale model testing in the UNH wave tank played a very important role in the SOWEC G-2 basic concept design and scale model fabrication. Simulation of wave conditions, test data collection and data analysis provided quantitative assessment of device performance. The scale model was easily modified to different configurations. Testing was done under various wave conditions, and test data were easily collected. The visible motion tracking system OPIE worked effectively to capture the structure motion for analysis.

The downward sloped bellows orientation was observed to produce higher efficiencies than either the horizontal or upward sloped orientation. The SOWEC G-2 testing program results indicated that the upward sloped bellows orientation produced the lowest efficiency and the horizontal orientation had an almost 5% greater efficiency than the upward orientation. The downward orientation made the highest efficiency (40.74% in peak pressure efficiency, 30.25% in average pressure efficiency) among all orientations.

The optimal configuration consisted of a 15 degrees downward sloped bellows orientation, the pressure plate center submerged 6 inches, a 1.5 second period wave forcing with a 0.351 meters wave height. Under these conditions, the SOWEC G-2 produced a peak pressure efficiency of 40.74% and an average pressure efficiency of 30.25%.

All enhancements, consisting of the kinetic control surface, extension plate and shoal plane, increased efficiencies. The results indicated that the enhancements made a great contribution to improving the SOWEC G-2 efficiency. The SOWEC G-2 captured sufficient energy only when the kinetic control surface was applied, and the extension plate made the efficiency increase about 3%.

5.2 Future Work

Future work on improving this device should include, in approximate order of importance:

- a. The next generation device SOWEC G-3 should include improvements discussed in section 4.6 for the SOWEC G-2. The issues include, but are not limited to, bellows stroke limitation, piston water pump, PTO pressure, restoring force system, and enhancement structure design. Meanwhile, model material and construction methods should also be considered.

- b. For testing in the UNH wave tank, the maximum scale of the next generation model could be $\frac{1}{4}$. The increased size would allow better prediction of full scale performance.

- c. A new full scale version should be considered in the future for open ocean testing. The full scale structure needs to be modified to adapt to ocean wave conditions. The fixed aluminum support frame have to replaced by a floating support consisting of two vertical hollow steel columns. A new PTO system should be developed with an air turbine, hydraulic, or rotary/linear generator system.

REFERENCES

Dean, R.G., Dalrymple, R.A. (1991) *Water Wave Mechanics for Engineers and Scientists*. World Scientific. River Edge, NJ. 353 p.

Michelin, D., Stott, S.(1997). *Optical Positioning Instrumentation and Evaluation*. Ocean Project Report. University of New Hampshire/University of Maine Seagrant. University of New Hampshire, Durham, NH. 85P.

U.S. Energy Information Administration.(2009). *Annual Energy review 2009, Tab 1.3*. Primary energy consumption by energy source, 1949-2009, 408 p.

John W. Twidell & Anthony D. Weir, (1986) *Renewable Energy Resources*. Taylor & Francis. NY. 581 p.

João Cruz. (2008) *Ocean Wave Energy: Current Status and Future Perspectives*. Springer, 431 p.

Salter S. Lin C. (1995) *The sloped IPS Wave Energy Converter*. 2nd European Wave Energy Conference Lisbon.

APPENDIX A: REGULAR WAVE MODEL TEST RESULTS

REGULAR WAVE SOWEC G-2 TEST RESULTS

Orientation	Frame Position	Period	Wave Height	Enhancements	Wave Power	Peak Capture Power	Average Capture power	Average efficiency	Peak Efficiency	Ob NO	Date
	Pin Location	T, (s)	H, (m)		We,(watt)	Wop,(watt)	Woa,(watt)	Zca	Zcp		
DOWNWARD	#5 & #1	2	0.287	KCS	101.005	8.691	7.043	5.60%	6.91%	18	8-Jun
DOWNWARD	#5 & #1	1.5	0.351	KCS	151.075	15.290	11.859	8.84%	11.40%	22	8-Jun
HORIZONTAL	#6 & #2	2	0.287	KCS	101.005	11.116	8.575	6.82%	8.84%	26	8-Jun
HORIZONTAL	#6 & #2	1.5	0.351	KCS	151.075	21.192	16.262	12.12%	15.80%	27	8-Jun
HORIZONTAL	#6 & #2	2	0.287	KCS	101.005	11.649	9.035	7.18%	9.26%	28	8-Jun
HORIZONTAL	#6 & #2	1.5	0.351	KCS	151.075	20.598	16.032	11.95%	15.35%	29	8-Jun
DOWNWARD	#6 & #2 (+2")	2	0.287	KCS	101.005	9.505	7.602	6.04%	7.56%	30	10-Jun
DOWNWARD	#6 & #2 (+2")	2	0.287	KCS	101.005	6.774	5.925	4.71%	5.39%	31	10-Jun
DOWNWARD	#6 & #2 (+2")	1.5	0.351	KCS	151.075	9.253	7.851	5.85%	6.90%	32	10-Jun
DOWNWARD	#6 & #2 (+2")	2.5	0.211	KCS	54.594	2.082	1.807	1.95%	2.25%	33	10-Jun
DOWNWARD	#6 & #2 (+2")	2	0.287	KCS	101.005	8.861	7.054	5.61%	7.05%	34	10-Jun
DOWNWARD	#6 & #2 (+1")	2	0.287	KCS	101.005	7.273	5.869	4.67%	5.78%	35	10-Jun
DOWNWARD	#6 & #2 (+1")	1.5	0.351	KCS	151.075	10.821	8.592	6.40%	8.07%	36	10-Jun
HORIZONTAL	#6 & #2 (+1")	2	0.287	KCS	101.005	8.923	7.090	5.64%	7.09%	37	10-Jun
DOWNWARD	#5 & #1	2	0.287	KCS	101.005	9.027	7.123	5.66%	7.18%	38	10-Jun
DOWNWARD	#5 & #1 (+3")	2	0.287	KCS	101.005	19.010	14.388	11.44%	15.12%	39	17-Jun
DOWNWARD	#5 & #1 (+3")	1.5	0.351	KCS	151.075	28.698	22.370	16.67%	21.39%	40	17-Jun
DOWNWARD	#5 & #1 (+3")	2.5	0.211	KCS	54.594	6.020	4.824	5.20%	6.49%	41	17-Jun
DOWNWARD	#5 & #1 (+3")	2.5	0.211	KCS	54.594	5.944	4.902	5.29%	6.41%	42	17-Jun
DOWNWARD	#5 & #1 (+3")	2	0.287	KCS	101.005	19.120	15.322	12.18%	15.20%	43	17-Jun
DOWNWARD	#5 & #1 (+3")	1.5	0.351	KCS	151.075	28.497	23.415	17.45%	21.24%	44	17-Jun
DOWNWARD	#5 & #1 (+3")	2.5	0.211	KCS	54.594	4.489	3.852	4.16%	4.84%	45	17-Jun
DOWNWARD	#5 & #1 (+3")	2	0.287	KCS	101.005	11.356	9.635	7.66%	9.03%	46	17-Jun
DOWNWARD	#5 & #1 (+3")	1.5	0.351	KCS	151.075	17.846	13.819	10.30%	13.30%	47	17-Jun
DOWNWARD	#5 & #1 (+4")	2.5	0.211	KCS	54.594	3.200	2.751	2.97%	3.45%	48	17-Jun
DOWNWARD	#5 & #1 (+4")	2	0.287	KCS	101.005	15.774	12.322	9.80%	12.54%	49	17-Jun
DOWNWARD	#5 & #1 (+4")	1.5	0.351	KCS	151.075	28.276	21.985	16.39%	21.08%	50	17-Jun
HORIZONTAL	#5 & #1 (+9")	2	0.287	KCS	101.005	11.711	9.148	7.27%	9.31%	51	17-Jun
HORIZONTAL	#5 & #1 (+9")	1.5	0.351	KCS	151.075	26.826	20.109	14.99%	19.99%	52	17-Jun
HORIZONTAL	#5 & #1 (+9")	2	0.287	KCS	101.005	14.000	10.787	8.58%	11.13%	53	17-Jun

REGULAR WAVE SOWEC G-2 TEST RESULTS

Orientation	Frame Position	Period	Wave Height	Enhancements	Wave Power	Peak Capture Power		Average Capture power	Average efficiency	Peak Efficiency		Ob NO.	Date
						Wp,(watt)	Woa,(watt)			Zca	Zcp		
	Pin Location	T, (s)	H, (m)		We,(watt)								
HORIZONTAL	#5 & #1 (+9")	1.5	0.351	KCS	151.075	35.691	24.796	18.48%	26.60%	54	17-Jun		
HORIZONTAL	#6 & #2 (+5")	2	0.287	KCS	101.005	18.738	13.969	11.11%	14.90%	55	17-Jun		
HORIZONTAL	#6 & #2 (+5")	2	0.287	KCS	101.005	24.637	18.555	14.75%	19.59%	56	17-Jun		
HORIZONTAL	#6 & #2 (+5")	1.5	0.351	KCS	151.075	48.580	36.069	26.88%	36.21%	57	17-Jun		
HORIZONTAL	#6 & #2 (+5")	2	0.287	KCS	101.005	19.349	14.347	11.41%	15.39%	59	17-Jun		
HORIZONTAL	#6 & #2 (+5")	1.5	0.351	KCS	151.075	35.567	25.862	19.28%	26.51%	60	17-Jun		
DOWNWARD	#6 & #2 (+0")	2	0.287	KCS	101.005	17.801	13.023	10.35%	14.15%	61	17-Jun		
DOWNWARD	#6 & #2 (+0")	2.5	0.211	KCS	54.594	4.125	3.686	3.98%	4.45%	62	17-Jun		
DOWNWARD	#6 & #2 (+0")	1.5	0.351	KCS	151.075	21.116	15.761	11.75%	15.74%	63	17-Jun		
DOWNWARD	#6 & #2 (+0")	2.5	0.211	KCS	54.594	4.798	4.197	4.53%	5.18%	64	17-Jun		
DOWNWARD	#6 & #2 (+0")	2	0.287	KCS	101.005	19.085	14.055	11.18%	15.18%	65	17-Jun		
DOWNWARD	#6 & #2 (+0")	1.5	0.351	KCS	151.075	23.613	17.741	13.22%	17.60%	66	17-Jun		
DOWNWARD	#6 & #2 (+0")	2.5	0.211	KCS	54.594	5.260	4.320	4.66%	5.67%	67	17-Jun		
DOWNWARD	#6 & #2 (+0")	2	0.287	KCS	101.005	22.744	17.328	13.78%	18.08%	68	17-Jun		
DOWNWARD	#6 & #2 (+0")	1.5	0.351	KCS	151.075	31.230	24.673	18.39%	23.28%	69	17-Jun		
DOWNWARD	#6 & #2 (+4")	2.5	0.211	KCS+EL	54.594	5.530	4.463	4.81%	5.97%	70	17-Jun		
DOWNWARD	#6 & #2 (+4")	2	0.287	KCS+EL	101.005	33.963	24.416	19.41%	27.00%	71	17-Jun		
HORIZONTAL	#6 & #2	2.5	0.211	KCS+EL	54.594	5.795	4.728	5.10%	6.25%	73	21-Jun		
DOWNWARD	#6 & #2	2.5	0.211	KCS+EL	54.594	7.899	6.020	6.49%	8.52%	76	21-Jun		
DOWNWARD	#6 & #2	2	0.287	KCS+EL	101.005	30.381	21.965	17.47%	24.16%	77	21-Jun		
DOWNWARD	#6 & #2	1.5	0.351	KCS+EL	151.075	37.895	27.707	20.65%	28.25%	78	21-Jun		
DOWNWARD	#6 & #2	2.5	0.211	KCS+EL	54.594	7.610	5.853	6.31%	8.21%	79	21-Jun		
DOWNWARD	#6 & #2	2	0.287	KCS+EL	101.005	24.637	17.428	13.86%	19.59%	80	21-Jun		
DOWNWARD	#6 & #2	1.5	0.351	KCS+EL	151.075	27.131	19.632	14.63%	20.22%	81	21-Jun		
DOWNWARD	#6 & #2	2.5	0.211	KCS+EL	54.594	6.855	5.346	5.77%	7.40%	82	21-Jun		
DOWNWARD	#6 & #2	2	0.287	KCS+EL	101.005	24.132	17.171	13.65%	19.19%	83	21-Jun		
DOWNWARD	#6 & #2	1.5	0.351	KCS+EL	151.075	32.496	23.360	17.41%	24.22%	84	21-Jun		
DOWNWARD	#5 & #1	2.5	0.211	KCS+EL	54.594	6.734	5.301	5.72%	7.26%	85	21-Jun		
DOWNWARD	#5 & #1	2	0.287	KCS+EL	101.005	23.967	17.299	13.75%	19.06%	86	21-Jun		

REGULAR WAVE SOWEC G-2 TEST RESULTS

Orientation	Frame Position	Period	Wave Height	Enhancements	Wave Power	Peak Capture Power	Average Capture power	Average efficiency	Peak Efficiency	Ob NO.	Date
	Pin Location		T, (s)		H, (m)	We,(watt)	Wop,(watt)	Woa,(watt)	Zca		
DOWNWARD	#5 & #1	1.5	0.351	KCS+EL	151.075	33.832	24.731	18.43%	25.22%	87	21-Jun
DOWNWARD	#5 & #1	2.5	0.211	KCS+EL	54.594	6.146	4.895	5.28%	6.63%	88	21-Jun
DOWNWARD	#5 & #1	2	0.287	KCS+EL	101.005	26.911	20.033	15.93%	21.40%	89	21-Jun
DOWNWARD	#5 & #1	1.5	0.351	KCS+EL	151.075	36.063	27.286	20.34%	26.88%	90	21-Jun
DOWNWARD	#5 & #1	2	0.287	KCS+EL	101.005	29.456	21.919	17.43%	23.42%	91	21-Jun
HORIZONTAL	#6 & #2	2	0.287	KCS+EL	101.005	23.741	17.674	14.05%	18.88%	96	1-Jul
HORIZONTAL	#6 & #2	1.5	0.351	KCS+EL	151.075	33.057	24.441	18.22%	24.64%	97	1-Jul
HORIZONTAL	#6 & #2	2	0.287	KCS+EL	101.005	29.321	22.016	17.51%	23.31%	98	1-Jul
HORIZONTAL	#6 & #2	1.5	0.351	KCS+EL	151.075	30.189	22.217	16.56%	22.50%	99	1-Jul
HORIZONTAL	#6 & #2	2	0.287	KCS+EL	101.005	23.422	16.968	13.49%	18.62%	100	1-Jul
HORIZONTAL	#6 & #2	1.5	0.351	KCS+EL	151.075	44.893	31.947	23.81%	33.46%	101	1-Jul
HORIZONTAL	#6 & #2	2.5	0.211	KCS+EL	54.594	11.891	8.821	9.52%	12.83%	102	1-Jul
HORIZONTAL	#6 & #2	2.5	0.211	KCS+EL	54.594	12.252	9.035	9.75%	13.22%	103	1-Jul
HORIZONTAL	#6 & #2	2	0.287	KCS+EL	101.005	26.146	18.609	14.80%	20.79%	104	1-Jul
HORIZONTAL	#6 & #2	1.5	0.351	KCS+EL	151.075	37.805	26.652	19.87%	28.18%	105	1-Jul
DOWNWARD	#6 & #2	2	0.287	KCS+EL	101.005	26.469	18.947	15.07%	21.05%	106	1-Jul
DOWNWARD	#6 & #2	2.5	0.211	KCS+EL	54.594	10.528	7.967	8.60%	11.36%	107	1-Jul
DOWNWARD	#6 & #2	2	0.287	KCS+EL	101.005	27.326	20.141	16.01%	21.73%	108	1-Jul
DOWNWARD	#6 & #2	2	0.287	KCS+EL	101.005	27.698	20.862	16.59%	22.02%	109	1-Jul
DOWNWARD	#6 & #2	1.5	0.351	KCS+EL	151.075	28.828	23.008	17.15%	21.49%	110	1-Jul
HORIZONTAL	#6(+7.5)	2	0.287	KCS+EL	101.005	15.320	11.591	9.22%	12.18%	111	20-Jul
HORIZONTAL	#6(+7.5)	2	0.287	KCS+EL	101.005	17.801	13.415	10.67%	14.15%	112	20-Jul
HORIZONTAL	#6(+7.5)	2.5	0.211	KCS+EL	54.594	8.188	6.283	6.78%	8.83%	113	20-Jul
HORIZONTAL	#6(+7.5)	1.5	0.351	KCS+EL	151.075	23.980	17.857	13.31%	17.87%	114	20-Jul
HORIZONTAL	#6(+7.5)	2	0.287	KCS+EL	101.005	20.598	15.034	11.95%	16.38%	115	20-Jul
HORIZONTAL	#6(+7.5)	2.5	0.211	KCS+EL	54.594	10.793	8.121	8.76%	11.64%	116	20-Jul

REGULAR WAVE SOWEC G-2 TEST RESULTS

Orientation	Frame Position	Period	Wave Height	Enhancements	Wave Power	Peak Capture Power	Average Capture power	Average efficiency	Peak Efficiency	Ob NO.	Date
	Pin Location	T, (s)	H, (m)		We,(watt)	Wop,(watt)	Woa,(watt)	Zca	Zcp		
HORIZONTAL	#6(+7.5)	1.5	0.351	KCS+EL	151.075	22.890	16.583	12.36%	17.06%	117	20-Jul
HORIZONTAL	#6(+7.5)	2	0.287	KCS+EL	101.005	22.371	16.609	13.21%	17.79%	118	20-Jul
HORIZONTAL	#6(+7.5)	2.5	0.211	KCS+EL	54.594	11.337	8.698	9.38%	12.23%	119	20-Jul
HORIZONTAL	#6(+7.5)	1.5	0.351	KCS+EL	151.075	26.413	19.750	14.72%	19.69%	120	20-Jul
HORIZONTAL	#7(+3.5)	2	0.287	KCS+EL	101.005	25.921	18.591	14.78%	20.61%	121	20-Jul
HORIZONTAL	#7(+3.5)	2.5	0.211	KCS+EL	54.594	9.902	7.492	8.08%	10.68%	122	20-Jul
HORIZONTAL	#7(+3.5)	1.5	0.351	KCS+EL	151.075	21.213	15.876	11.83%	15.81%	123	20-Jul
HORIZONTAL	#7(+3.5)	2	0.287	KCS+EL	101.005	28.302	20.346	16.18%	22.50%	124	20-Jul
HORIZONTAL	#7(+3.5)	2.5	0.211	KCS+EL	54.594	12.362	9.166	9.89%	13.34%	125	20-Jul
HORIZONTAL	#7(+3.5)	1.5	0.351	KCS+EL	151.075	27.835	20.881	15.56%	20.75%	126	20-Jul
HORIZONTAL	#7(+3.5)	2	0.287	KCS+EL	101.005	23.592	16.888	13.43%	18.76%	127	20-Jul
HORIZONTAL	#7(+3.5)	2.5	0.211	KCS+EL	54.594	11.542	8.620	9.30%	12.45%	128	20-Jul
HORIZONTAL	#7(+3.5)	1.5	0.351	KCS+EL	151.075	23.422	17.442	13.00%	17.46%	129	20-Jul
HORIZONTAL	#7(+3.5)	2	0.287	KCS+EL	101.005	20.583	14.928	11.87%	16.37%	130	20-Jul
HORIZONTAL	#7(+3.5)	2.5	0.211	KCS+EL	54.594	10.604	8.037	8.67%	11.44%	131	20-Jul
HORIZONTAL	#6(+3.5)	2.5	0.211	KCS+EL	54.594	16.144	12.100	13.05%	17.42%	132	28-Jul
HORIZONTAL	#6(+3.5)	2	0.287	KCS+EL	101.005	37.895	27.412	21.80%	30.13%	133	28-Jul
HORIZONTAL	#6(+3.5)	1.5	0.351	KCS+EL	151.075	52.586	38.598	28.77%	39.20%	134	28-Jul
HORIZONTAL	#6(+3.5)	2.5	0.211	KCS+EL	54.594	13.560	10.380	11.20%	14.63%	135	28-Jul
HORIZONTAL	#6(+3.5)	2	0.287	KCS+EL	101.005	30.429	21.822	17.35%	24.20%	136	28-Jul
HORIZONTAL	#6(+3.5)	1.5	0.351	KCS+EL	151.075	44.161	31.519	23.49%	32.92%	137	28-Jul
DOWNWARD	#5 & #1	2.5	0.211	KCS+EL	54.594	12.199	9.026	9.74%	13.16%	138	28-Jul
DOWNWARD	#5 & #1	2	0.287	KCS+EL	101.005	27.802	20.083	15.97%	22.11%	139	28-Jul
DOWNWARD	#5 & #1	1.5	0.351	KCS+EL	151.075	50.289	37.544	27.98%	37.48%	140	28-Jul
DOWNWARD	#5 & #1	2.5	0.211	KCS+EL	54.594	12.732	9.769	10.54%	13.74%	141	28-Jul
DOWNWARD	#5 & #1	2	0.287	KCS+EL	101.005	35.038	24.308	19.33%	27.86%	142	28-Jul
DOWNWARD	#5 & #1	1.5	0.351	KCS+EL	151.075	45.327	34.253	25.53%	33.78%	143	28-Jul
DOWNWARD	#5 & #1	2.5	0.211	KCS+EL	54.594	12.174	9.239	9.97%	13.13%	144	28-Jul
DOWNWARD	#5 & #1	2	0.287	KCS+EL	101.005	30.386	22.115	17.58%	24.16%	145	28-Jul
DOWNWARD	#5 & #1	1.5	0.351	KCS+EL	151.075	37.660	28.105	20.95%	28.07%	146	28-Jul

REGULAR WAVE SOWEC G-2 TEST RESULTS

Orientation	Frame Position	Period	Wave Height		Enhancements	Wave Power	Peak Capture Power	Average Capture power	Average efficiency	Peak Efficiency	Ob NO.	Date
	Pin Location		T _p (s)	H _p (m)		W _e (watt)	W _{op} (watt)	W _{oa} (watt)	Z _{ca}	Z _{cp}		
DOWNWARD	#5 & #1	2.5	0.211		KCS+EL	54.594	12.923	9.853	10.63%	13.94%	147	28-Jul
DOWNWARD	#5 & #1	2	0.287		KCS+EL	101.005	26.469	19.405	15.43%	21.05%	148	28-Jul
DOWNWARD	#5 & #1	1.5	0.351		KCS+EL	151.075	41.965	30.973	23.09%	31.28%	149	28-Jul
DOWNWARD	#5 & #1	2.5	0.211		KCS+EL	54.594	13.297	10.325	11.14%	14.35%	150	28-Jul
DOWNWARD	#5 & #1	2	0.287		KCS+EL	101.005	34.939	25.554	20.32%	27.78%	151	28-Jul
DOWNWARD	#5 & #1	1.5	0.351		KCS+EL	151.075	54.652	40.578	30.25%	40.74%	152	28-Jul
DOWNWARD	#6(+0)	2.5	0.211		KCS+EL	54.594	8.796	6.773	7.31%	9.49%	153	28-Jul
DOWNWARD	#6(+0)	2	0.287		KCS+EL	101.005	28.870	20.924	16.64%	22.96%	154	28-Jul
DOWNWARD	#6(+0)	1.5	0.351		KCS+EL	151.075	35.750	27.000	20.13%	26.65%	155	28-Jul
DOWNWARD	#6(+0)	2.5	0.211		KCS+EL	54.594	7.706	6.040	6.52%	8.31%	156	28-Jul
DOWNWARD	#6(+0)	2	0.287		KCS+EL	101.005	19.356	14.237	11.32%	15.39%	157	28-Jul
DOWNWARD	#6(+2)	2.5	0.211		KCS+EL	54.594	10.022	7.637	8.24%	10.81%	158	28-Jul
DOWNWARD	#6(+2)	2	0.287		KCS+EL	101.005	23.980	17.459	13.88%	19.07%	159	28-Jul
DOWNWARD	#6(+2)	2.5	0.211		KCS+EL	54.594	11.420	8.726	9.41%	12.32%	160	28-Jul
DOWNWARD	#6(+2)	2	0.287		KCS+EL	101.005	29.101	21.160	16.83%	23.14%	161	28-Jul
DOWNWARD	#6(+2)	1.5	0.351		KCS+EL	151.075	38.837	29.240	21.79%	28.95%	162	28-Jul
HORIZONTAL	#6(+5)	2	0.287		KCS	101.005	34.658	25.141	19.99%	27.56%	163	3-Aug
HORIZONTAL	#6(+5)	1.5	0.351		KCS	151.075	49.601	36.534	27.23%	36.97%	164	3-Aug
HORIZONTAL	#6(+5)	2.5	0.211		KCS	54.594	15.615	11.889	12.83%	16.85%	165	3-Aug
DOWNWARD	#5	2	0.287		KCS	101.005	28.746	21.399	17.02%	22.86%	166	3-Aug
DOWNWARD	#5	1.5	0.351		KCS	151.075	42.252	33.123	24.69%	31.49%	167	3-Aug
DOWNWARD	#5	2.5	0.211		KCS	54.594	13.461	10.715	11.56%	14.52%	168	3-Aug
DOWNWARD	#5	2	0.287		KCS	101.005	28.999	22.711	18.06%	23.06%	169	3-Aug
DOWNWARD	#5	1.5	0.351		KCS	151.075	40.599	32.114	23.94%	30.26%	170	3-Aug
DOWNWARD	#5	2.5	0.211		KCS	54.594	12.882	10.384	11.20%	13.90%	171	3-Aug
HORIZONTAL	#6	2	0.287		KCS	101.005	30.278	23.442	18.64%	24.08%	172	3-Aug
HORIZONTAL	#6	1.5	0.351		KCS	151.075	47.082	36.061	26.88%	35.09%	173	3-Aug
HORIZONTAL	#6	2	0.287		KCS	101.005		#VALUE!	#VALUE!	0.00%	174	3-Aug
HORIZONTAL	#6	2	0.287		KCS	101.005	28.828	20.981	16.68%	22.92%	175	3-Aug
HORIZONTAL	#6	2.5	0.211		KCS	54.594	12.519	9.771	10.54%	13.51%	176	3-Aug
HORIZONTAL	#6	1.5	0.351		KCS	151.075	36.198	26.719	19.92%	26.98%	177	3-Aug

REGULAR WAVE SOWEC G-2 TEST RESULTS

Orientation	Frame Position	Period	Wave Height	Enhancements	Wave Power	Peak Capture Power	Average Capture power	Average efficiency	Peak Efficiency	Ob NO.	Date
	Pin Location	T, (s)	H, (m)		W _e , (watt)	W _{op} , (watt)	W _{oa} , (watt)	Z _{ca}	Z _{cp}		
HORIZONTAL	#6	2	0.287	KCS	101.005	22.156	8.229	6.54%	17.62%	178	3-Aug
HORIZONTAL	#6	2.5	0.211	KCS	54.594	13.533	10.239	11.05%	14.60%	179	3-Aug
HORIZONTAL	#6	2	0.287	KCS	101.005	30.141	22.429	17.83%	23.97%	180	3-Aug
HORIZONTAL	#6	1.5	0.351	KCS	151.075	41.992	31.409	23.41%	31.30%	181	3-Aug
DOWNWARD	#5	2.5	0.211	KCS+EL+SL	54.594	14.834	11.383	12.28%	16.00%	182	12-Aug
DOWNWARD	#5	2.5	0.211	KCS+EL+SL	54.594	13.813	10.683	11.53%	14.90%	183	12-Aug
DOWNWARD	#5	2.2	0.254	KCS+EL+SL	79.113	20.198	14.938	13.29%	17.97%	184	12-Aug
DOWNWARD	#5	2.2	0.254	KCS+EL+SL	79.113	21.340	16.144	14.37%	18.99%	185	12-Aug
DOWNWARD	#5	2	0.287	KCS+EL+SL	101.005	35.991	27.283	21.69%	28.62%	186	12-Aug
DOWNWARD	#5	2.5	0.211	KCS+EL+SL	54.594	17.602	13.364	14.42%	18.99%	187	12-Aug
DOWNWARD	#5	2.2	0.254	KCS+EL+SL	79.113	28.904	21.272	18.93%	25.72%	188	12-Aug
DOWNWARD	#5	2.5	0.211	KCS+EL+SL	54.594	14.608	11.161	12.04%	15.76%	189	12-Aug
DOWNWARD	#5	2.2	0.254	KCS+EL+SL	79.113	27.496	20.144	17.93%	24.47%	190	12-Aug
HORIZONTAL	#6	2.5	0.211	KCS+EL+SL	54.594	14.138	10.022	10.81%	15.25%	191	16-Aug
HORIZONTAL	#6	2	0.287	KCS+EL+SL	101.005	27.105	18.944	15.06%	21.55%	192	16-Aug
HORIZONTAL	#6	2.5	0.211	KCS+EL+SL	54.594	15.231	11.558	12.47%	16.43%	193	16-Aug
HORIZONTAL	#6	2	0.287	KCS+EL+SL	101.005	28.904	21.830	17.36%	22.98%	194	16-Aug
HORIZONTAL	#6	2.2	0.254	KCS+EL+SL	79.113	26.389	19.814	17.63%	23.49%	195	16-Aug
HORIZONTAL	#6	2.2	0.254	KCS+EL+SL	79.113	17.276	12.696	11.30%	15.37%	196	16-Aug
HORIZONTAL	#6	2.5	0.211	KCS+EL+SL	54.594	16.184	11.193	12.08%	17.46%	197	16-Aug
HORIZONTAL	#6	2.2	0.254	KCS+EL+SL	79.113	36.435	24.336	21.66%	32.43%	198	16-Aug
HORIZONTAL	#6	2	0.287	KCS+EL+SL	101.005	36.350	24.445	19.44%	28.90%	199	16-Aug
DOWNWARD	#6	2.5	0.211	KCS+EL+SL	54.594	24.301	16.348	17.64%	26.22%	200	16-Aug
DOWNWARD	#6	2.2	0.254	KCS+EL+SL	79.113	45.522	30.225	26.90%	40.51%	201	16-Aug
DOWNWARD	#6	2.5	0.211	KCS+EL+SL	54.594	17.737	11.960	12.90%	19.14%	202	16-Aug
DOWNWARD	#6	2.5	0.211	KCS+EL+SL	54.594	21.648	14.550	15.70%	23.35%	203	16-Aug
HORIZONTAL	#7	2.5	0.211	KCS+EL+SL	54.594	22.422	15.223	16.42%	24.19%	204	17-Aug
HORIZONTAL	#7	2.2	0.254	KCS+EL+SL	79.113	39.595	26.585	23.66%	35.24%	205	17-Aug
HORIZONTAL	#7	2.5	0.211	KCS+EL+SL	54.594	23.666	16.176	17.45%	25.53%	206	17-Aug
HORIZONTAL	#7	2.2	0.254	KCS+EL+SL	79.113	38.154	25.588	22.77%	33.95%	207	17-Aug
HORIZONTAL	#7	2	0.287	KCS+EL+SL	101.005	43.477	29.035	23.09%	34.57%	208	17-Aug
DOWNWARD	#6	2.5	0.211	KCS+EL+SL	54.594	35.538	23.757	25.63%	38.34%	209	17-Aug
DOWNWARD	#6	2.2	0.254	KCS+EL+SL	79.113	44.046	29.248	26.03%	39.20%	210	17-Aug
DOWNWARD	#6	2.5	0.211	KCS+EL+SL	54.594	26.271	17.674	19.07%	28.34%	211	17-Aug
DOWNWARD	#6	2.2	0.254	KCS+EL+SL	79.113	46.980	31.304	27.86%	41.81%	212	17-Aug
DOWNWARD	#6	2.5	0.211	KCS+EL+SL	54.594	24.984	16.905	18.24%	26.95%	213	17-Aug
DOWNWARD	#6	2.5	0.211	KCS+EL+SL	54.594	24.359	16.425	17.72%	26.28%	214	17-Aug
DOWNWARD	#6	2.5	0.211	KCS+EL+SL	54.594	20.783	14.237	15.36%	22.42%	215	17-Aug
DOWNWARD	#6	2.2	0.254	KCS+EL+SL	79.113	40.443	27.089	24.11%	35.99%	216	17-Aug
DOWNWARD	#6	2.5	0.211	KCS+EL+SL	54.594	12.899	9.349	10.09%	13.92%	217	17-Aug
DOWNWARD	#6	2.5	0.211	KCS+EL+SL	54.594	14.138	10.022	10.81%	15.25%	218	17-Aug
DOWNWARD	#6	2.5	0.211	KCS+EL+SL	54.594	8.648	6.077	6.56%	9.33%	219	17-Aug

APPENDIX B: SURFACE ELEVATION MEASURED BY WAVE STAFF

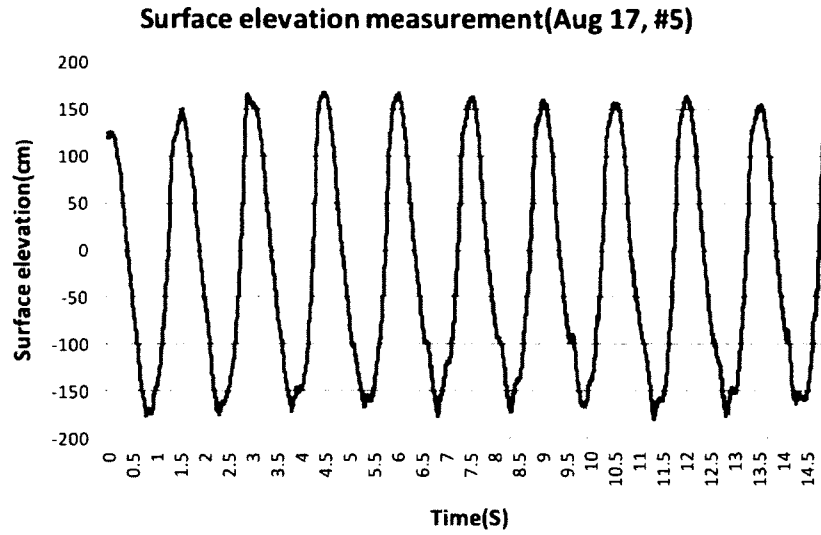


Fig 0.1: Surface Elevation for 1.5s Period Wave with 0.351m Wave Height

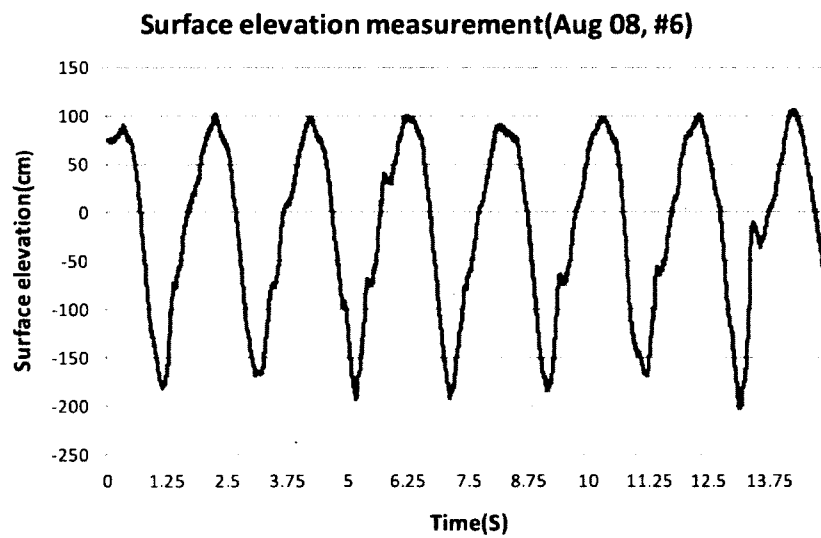


Fig 0.2: Surface Elevation for 2.0s Period Wave with 0.287m Wave Height

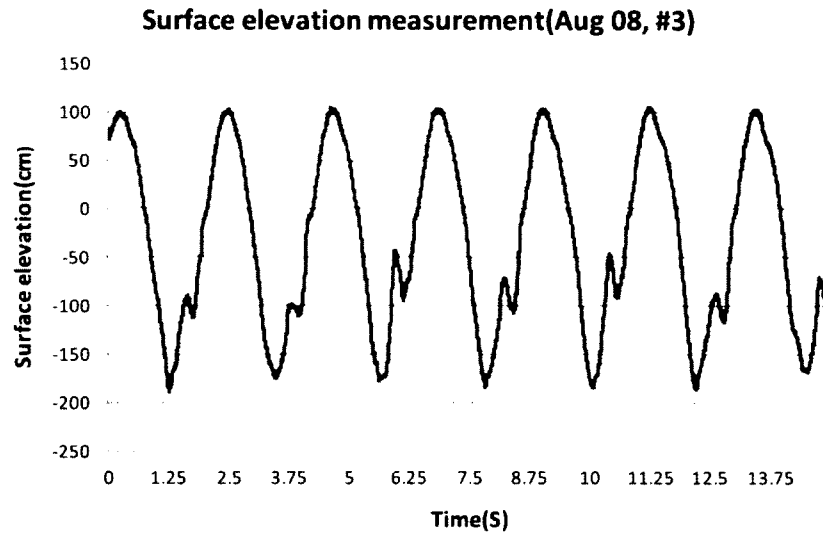


Fig 0.3: Surface Elevation for 2.2s Period Wave with 0.254m Wave Height

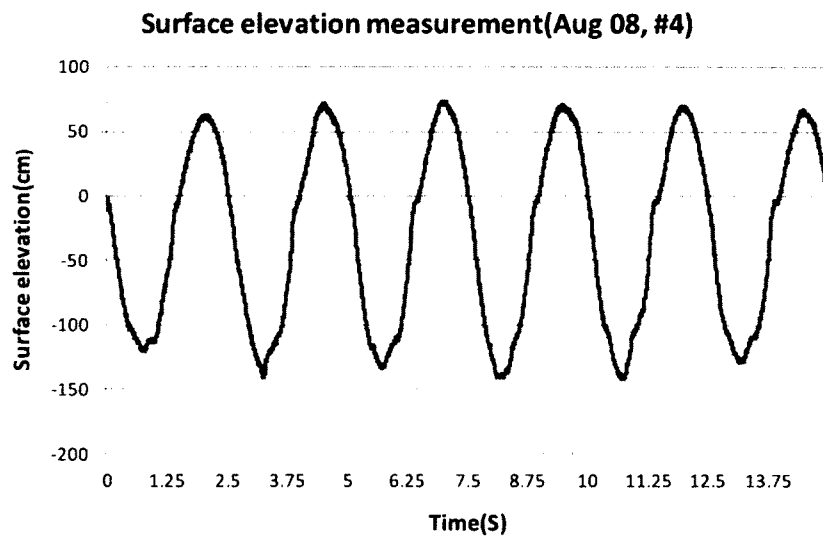


Fig 0.4: Surface Elevation for 2.5s Period Wave with 0.211m Wave Height